Integration of membrane filtration with thermocatalysis for water purification

Janowska, Katarzyna Joanna

DOI (link to publication from Publisher):
10.54337/aau510739165

Publication date:
2022

Document Version
Publisher's PDF, also known as Version of record

INTEGRATION OF MEMBRANE FILTRATION WITH THERMOCATALYSIS FOR WATER PURIFICATION

BY
KATARZYNA JOANNA JANOWSKA

DISSERTATION SUBMITTED 2022

AALBORG UNIVERSITY
DENMARK

INTEGRATION OF MEMBRANE FILTRATION WITH THERMOCATALYSIS FOR WATER PURIFICATION

BY
KATARZYNA JOANNA JANOWSKA

AALBORG UNIVERSITY
DENMARK

DISSERTATION SUBMITTED 2022

Dissertation submitted: September 2022

PhD supervisor: Associate Professor Vittorio Boffa
Aalborg University

PhD committee: Associate Professor Jens Muff (chair)
Aalborg University, Denmark

Assistant Professor Irina Petrinic
University of Maribor, Slovenia

Professor Vassilis Stathopoulos
National and Kapodistrian University of Athens, Greece

PhD Series: Faculty of Engineering and Science, Aalborg University

Department: Department of Chemistry and Bioscience

ISSN (online): 2446-1636
ISBN (online): 978-87-7573-810-6

Published by:
Aalborg University Press
Kroghstræde 3
DK – 9220 Aalborg Ø
Phone: +45 99407140
aauf@forlag.aau.dk
forlag.aau.dk

Printed in Denmark by Stibo Complete, 2022

ACKNOWLEDGMENTS

This thesis has been submitted for assessment in partial fulfillment of the PhD degree. The thesis is based on published and submitted scientific papers listed at the end of this work. Most of project was hold at Section of Chemistry at Aalborg University from March 2018 to July 2022. Part of the work was conducted in the form of secondments at University of Turin from May 2018 – June 2018, at company IRIS in July 2018, at University of Piedmont Orientale in February 2019 and at Liqtech A/S in March-June 2021. This study is a part of the European Union's Horizon 2020 research and innovation programme Aquality under the Marie Skłodowska-Curie EU funding.

First of all, I would like to thank my supervisors Vittorio Boffa, Mads Koustrup-Jørgensen and Victor M. Candelario for their support and guidance throughout my PhD project. I appreciate your patience and professionalism in discussing new experiments, results, and manuscripts. Thank you for all the time that you found for answering my scientific questions and solving problems.

I would like to thank all my collaborators who helped me to realize the goal of my studies through their scientific experience and expertise. Special thanks to Professor Giuliana Magnacca and Professor Debora Fabri for guidance and supervision during my stay at University of Turin.

I would like to thank all the ESRs and members of AQUAlity project for fruitful cooperation and the opportunity to share experience and discover your research during project meetings and work in work packages. Special thanks to Fabricio and Esra for all the support and friendship.

Thank you to all present and former colleagues from the Section of Chemistry and Biotechnology at Aalborg University that I met throughout the duration of my PhD studies. I would like to highlight Malwina, Martin, Max, Kacper, Chao, Tobias, Usuma, Yang, Mikkel, Søren, Rasmus, Zhencai, Chengwei, Ang, Pengfei, Tao, Xiangting, Kamila, Katie, Marta, Giulia, Anne-Sophie.

A special thanks go to my family, to my parents, Anna and Wojciech for believing in me and supporting me in all my actions and decisions, and to my partner who was always patient and understanding.

Finally, a very special thanks to my daughters Maja and Lucy who were born during my PhD, significantly extending my scientific journey. You taught me that nothing is impossible and motivated me to reach my goals. I hope that one day you can read this PhD thesis and get inspired to find new solutions to solve problems of the future world.

TABLE OF CONTENTS

CHAPTER 1. INTRODUCTION

In the World Economic Forum 2019, the scarcity of fresh water has been recognized as one of the largest global risks in terms of potential impact over the next decade [1]. Global water scarcity crisis requires strategies for water purification and reusage. However, conventional physicochemical and biological wastewater treatment plants (WWTPs) reveal their inefficiency on the complete removal of organic contaminants causing their potential release in the natural water bodies and in the environment [2]. Among them are contaminants of emerging concern (CECs) which even though are present in trace amounts, have especially hazardous effect on environment and human health. Therefore, there is a need for more powerful water treatment technologies. The integration of membrane filtration with advanced oxidation processes (AOPs) is a unique and highly innovative hybrid green technology for environmentally sustainable removal of CECs from aqueous systems which is of interest for further research.

1.1. CONTAMINANTS OF EMERGING CONCERN

In recent years, rapid growth of agriculture, industrialization, and urbanization, has caused increase of the occurrence of CECs which are recognized as a worldwide concern as they are suspected to have or have demonstrated adverse effects on human and wildlife endocrine system. CECs can include unknown, newly discovered or previously recognized compounds such as pharmaceuticals, personal care products, endocrine disruptors, surfactants, persistent organic contaminants, industrial chemicals, pesticides and artificial sweeteners [3]. The most common sources of CECs that end up in the municipality's sewage are shown in the Figure 1.

Conventional physicochemical and biological wastewater plants (WWTPs) are not effective in removal of all CECs, which are present at low concentration levels of ng/L to μg/L. Moreover, they are difficult to be traced due to requirement of specific detection methods and most analytical instruments are unable for directly detection of CECs [4]. Until now, the mostly used analytical techniques available to detect CECs are liquid and gas chromatography coupled with mass spectrometry (respectively LC-MS and GC-MS) due to its high selectivity, sensitivity and specificity [5], inductively coupled plasma mass spectrometry (ICP-MS) [6] due to its high-throughput capability and the ability to characterize a wide range of nanoparticles, solid phase extraction liquid chromatography mass spectrometry (SPE-LC-MS/MS) [7] and high performance liquid chromatography (HPLC) [8]. Triple quadrupole mass spectrometers provide selective monitoring of known (targeted) compounds demonstrating high sensitivity in complex environmental samples. For unknown (untargeted) compounds, high-resolution accurate-mass (HRAM) mass spectrometry can be used.

Furthermore, CECs elimination is not monitored due to lack of specific regulations. According to Global Water Research Coalition 44 compounds are classified as emerging contaminants in three main groups based on the following criteria: human toxicity, ecotoxicity, degradability, resistance to treatment and occurrence in the environment [9]. Endocrine disruptors and pharmaceuticals have been for the first time approved by Water Directive and included in the quality standards and watch list mechanism by the EU Council only in 2020 [10].

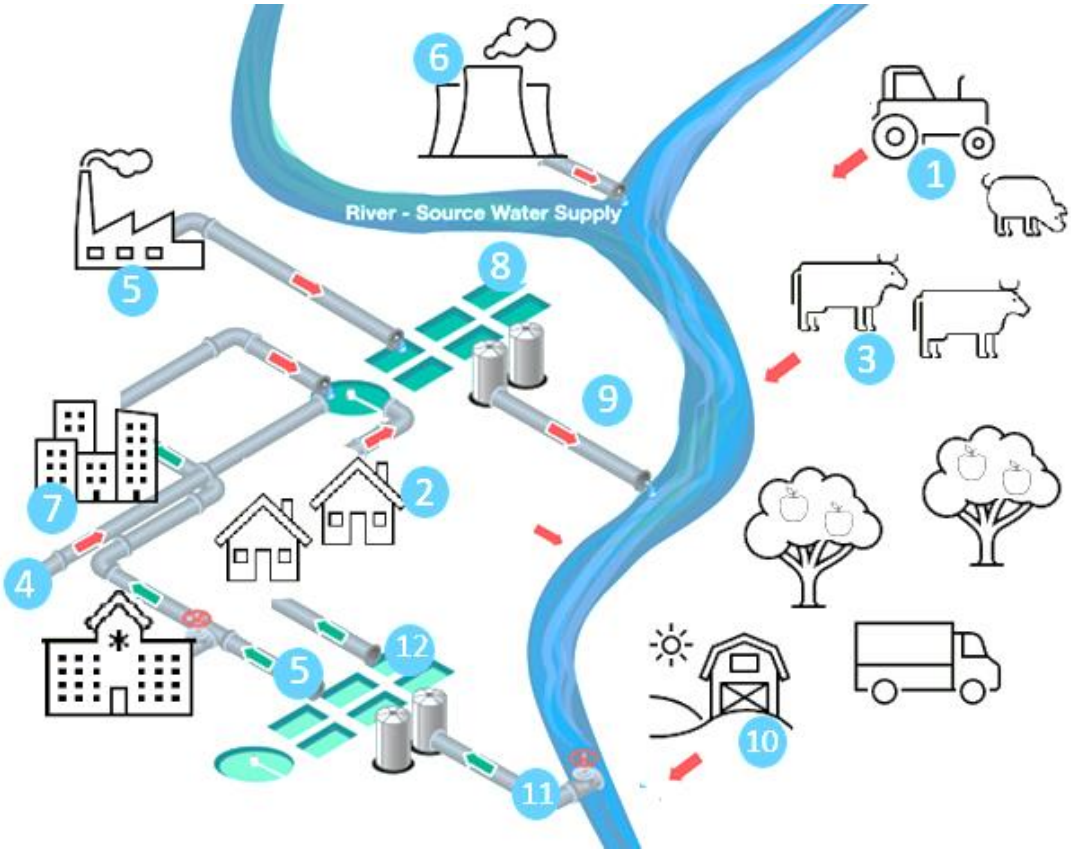

Figure 1. Sources of contaminants of emerging concern, where: 1 – agriculture pesticide runoff, 2 – residential runoff and effluent, 3 – farm and livestock runoff, 4 – hospital waste effluent, 5 – industrial runoff and effluent, 6 – energy generation effluent, 7 – urban runoff and effluent, 8 – wastewater treatment plant, 9 – wastewater effluent, 10 – septic tank affecting the underground water, 11 – drinking water intake, 12 – drinking water treatment plant.

1.2. METHODS OF WATER PURIFICATION

Water purification is the process of removing undesirable chemical compounds, organic and inorganic materials, biological contaminants, and gases from contaminated water in order to produce cleaner water for a specific purpose. The water purification methods are classified into physical, chemical, and biological. The most common physical methods are filtration, sedimentation, distillation and boiling. Chemical methods include adsorption, coagulation, flocculation, chlorination and ozonation. Other physical methods are based on electromagnetic radiations, such as ultraviolet light. Biological processes are based on slow sand filters and biologically active carbons [11]. A detailed classification of water purification methods is presented in Table 1.

Among the water purification methods, membrane technologies and advanced oxidation processes have recently gained attention in wastewater treatment as they combine process stability with improvement of effluent quality. Moreover, their integration as a hybrid process helps to achieve simultaneous retention and mineralization of CECs [12].

Table 1. Water purification methods.

CHEMICAL	PHYSICAL	BIOLOGICAL
• chemical oxidation • chemical precipitation • coagulation • dissolved air flotation • electrochemical oxidation • flocculation • hydrolysis • neutralization • solvent extraction • ion exchange	• adsorption • distillation • filtration • steam stripping • oil and grease skimming • oil/water separation • sedimentation • membrane technologies	• biological nitrogen removal • bioaugmentation • activated sludge • extented aeration • anaerobic processes • rotating biological contactors • sequencing batch reactors and tracking filters

1.3. ADVANCED OXIDATION PROCESSES

Advanced oxidation processes are based on the production of highly reactive hydroxyl species (ROSs), mainly hydroxyl radicals OH^- that are strong oxidizing agents and reactive electrophiles, which react with electron-rich organic compounds and mineralize them into CO_2 and inorganic ions [13]. There are four ways in which hydroxyl radicals attack organic pollutants: radical addition, hydrogen abstraction, electron transfer and radical combination. Through the reactions with organic compounds, they produce carbon-centered radicals (R· or R·–OH), which in assistance of O_2 can be further transformed into organic peroxyl radicals (ROO·). The further reaction of radicals ends as formation of more reactive species, such as H_2O_2 and super oxide ($O2^{\bullet-}$), that degrade and mineralize organic compounds [14].

Additionally, compared to conventional processes, the degradation of pollutants by AOPs occurs without generating a secondary waste stream. Based on the phase of the catalysts and the reaction mixture, AOPs can be classified into homogenous and heterogenous processes [11]. The classification of AOPs, which include photochemical degradation processes (UV/O_3, UV/H_2O_2), photocatalysis (TiO_2/UV, photo-Fenton reactives), and chemical oxidation processes (O_3, O_3/H_2O_2, H_2O_2/Fe^{2+}) [15], is presented in Figure 2.

Fenton processes are due to its advantages, such as simple operation, rapid degradation and mineralization, wide application range and strong anti-interface ability, the most popular oxidation processes used for wastewater treatment [16]. Production of $^{\bullet}OH$ radicals by Fenton reagent occurs in a simple way by the addition of hydrogen peroxide to iron salts as follows [17]:

$$Fe^{2+} + H_2O_2 \rightarrow Fe^{3+} + {}^{\bullet}OH + OH^- \quad (1)$$

Heterogeneous AOPs require the presence of a catalyst in combination with other systems such as ozone, hydrogen peroxide and light to perform the degradation of organic pollutants. Recently, the perovskite catalysts gained attention as they seem to be promising due to their high thermal stability, versatile composition, and generation of reactive oxygen species [18]. However, there are some limitations of perovskites in AOP systems such as small surface area, leaching of metal ions, or low number of active sites [19].

Another powerful oxidant used for the degradation of toxic organic pollutants is ozone (O_3) [20]. There are two oxidation mechanisms of ozone such as direct electrophilic attack by molecular ozone at low pH and indirect attack through the formation of hydroxyl radicals at basic pH [21]. The mechanism of $OH^{\cdot}$ generation is expressed as follows [14]:

$$3O_3 + H_2O \rightarrow 2\ {}^{\bullet}OH + 4O_2 \quad (2)$$

The combination of different AOPs has a synergistic effect as more oxidants are involved in the process. The hybrid allows also to improve the selectivity [22].

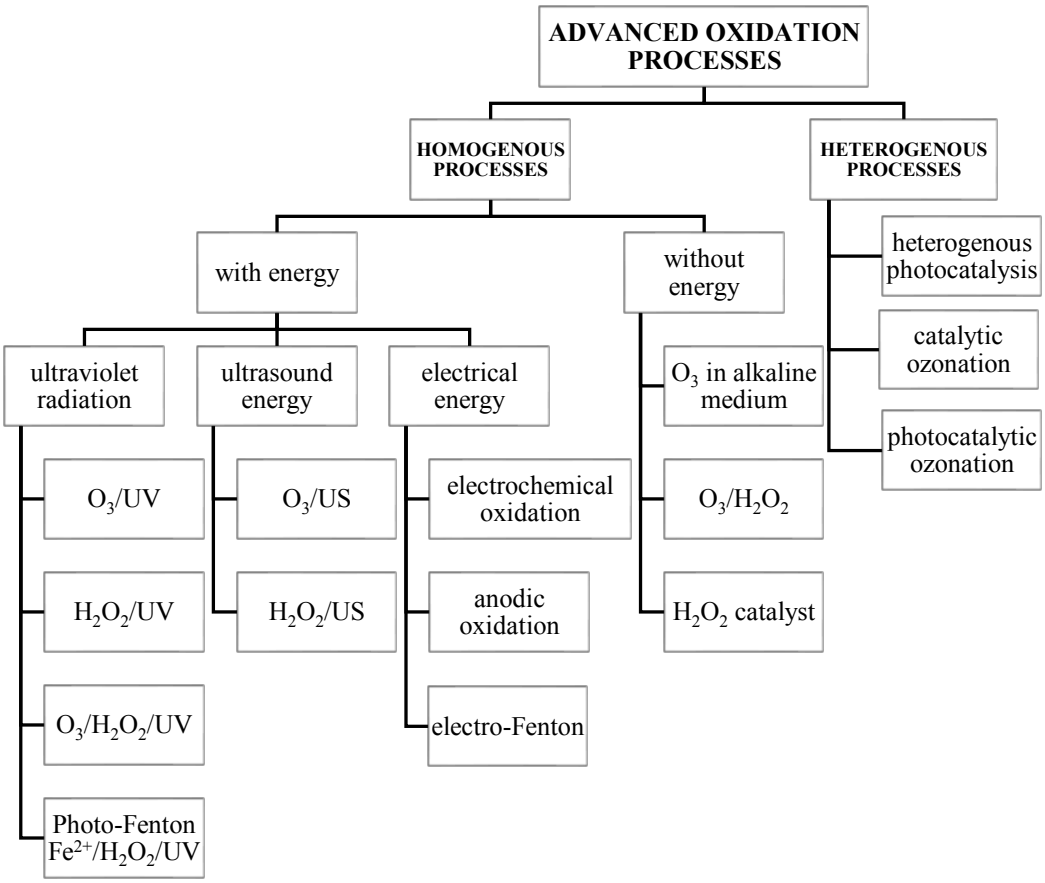

Figure 2. Classification of advanced oxidation processes, where O_3 – ozone, H_2O_2 – hydrogen peroxide, UV – ultraviolet radiation, US – ultrasound energy, Fe^{2+} - ferrous ion.

1.4. MEMBRANE FILTRATION PROCESSES

A membrane is a selective barrier that separates two phases and control transport of various compounds of a stream by sieving, diffusion or sorption allowing to pass smaller particles and retaining larger ones. Transport through a membrane is induced by the gradient across the membrane. The most common type of driving force is pressure gradient. For pressure-driven processes filtration occurs as an effect of pressure gradient created across the membrane. The driving forces for non-pressure driven processes are concentration, electrical power or temperature [23]. The classification of membrane processes divided into pressure and non-pressure driven processes is presented in the Figure 3:

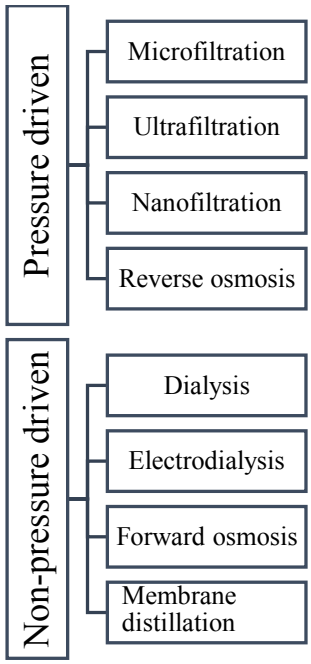

Figure 3. Membrane processes classification based on pressure gradient.

Depending on their application pressure driven membranes have different pore sizes. The smaller the pore size the higher the rejection. It has an influence on the decease of membrane fouling at the same time. Therefore, higher pressure is necessary to force permeate to pass through the smaller pores. The pore size distribution of different membrane process is showed in Figure 4.

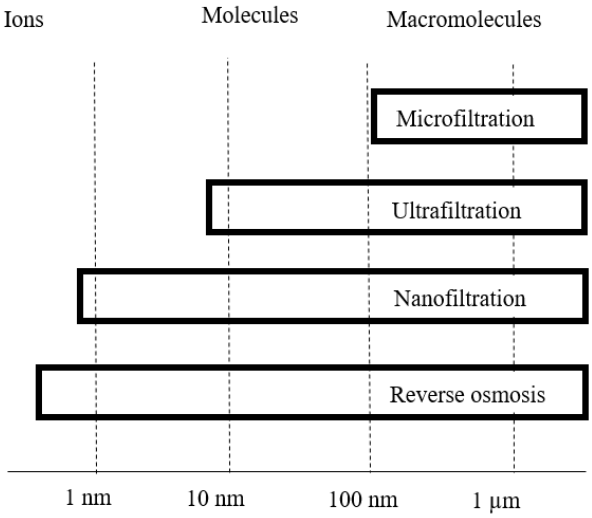

Figure 4. Different types of pressure-driven membranes and their filtering principles depending on the pore size.

There are many other ways of membrane classification depending on their nature, structure, geometry and transport mechanism (Figure 5) [24].

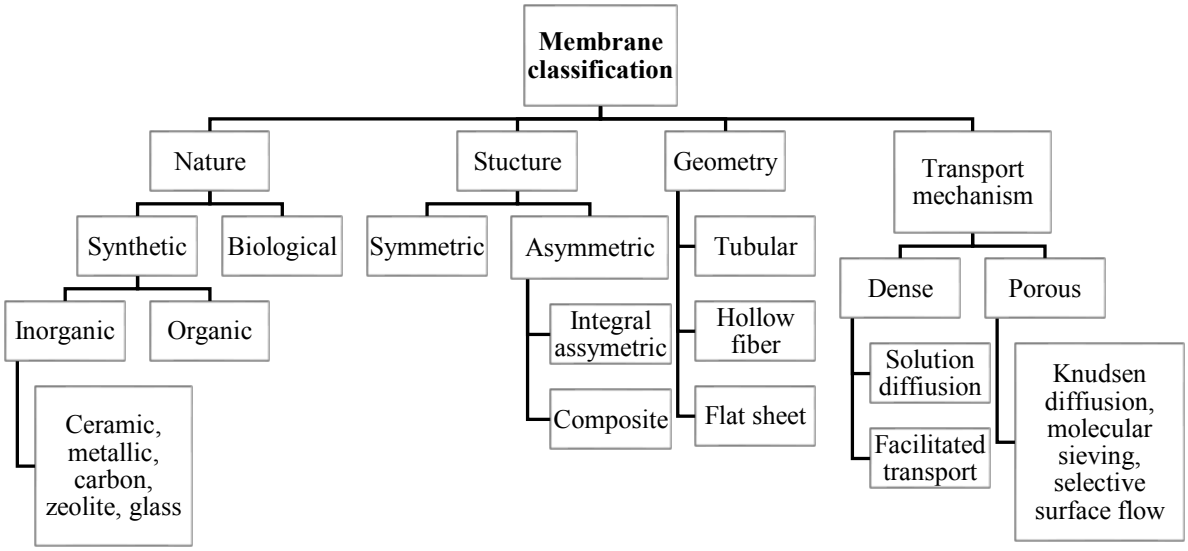

Figure 5. Membrane classification according to different criteria.

Membrane filtration can be operated in dead-end mode for batch production and in cross-flow for continuous operation. During the dead-end mode the feed flows perpendicular to the membrane. As all the water which is introduced to the system passes through the membrane, particles and other compounds accumulate and deposit on the membrane surface, forming a cake layer. This causes decrease of the flux over time. Periodic backwash is needed to eliminate the fouling and to reduce the flux. Otherwise, dead-end filtration requires regular membrane cleaning or membrane replacement. Principle of dead-end filtration is showed in Figure 6 [25].

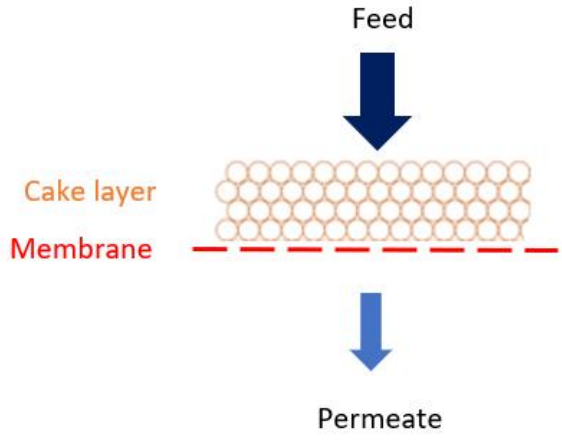

Figure 6. Scheme of dead-end filtration.

During the cross-flow filtration the feed flows tangentially to the membrane surface. Retentate passes along the membrane surface and back to the feed tank for recirculation. Permeate passes across the membrane. In cross-flow filtration the flux remain higher as the retained material is continuously removed by the stream. The main application of cross-flow is to concentrate the feed [26],[27]. The process is presented in Figure 7.

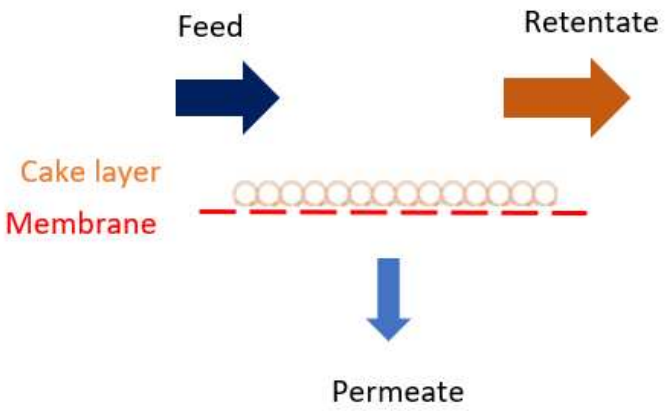

Figure 7. Scheme of cross-flow filtration.

Membrane technology used in wastewater treatment for separation and retention of suspended and colloidal solids and pathogens usually involves microfiltration (MF) or ultrafiltration (UF) units. The membranes are introduced into the biological wastewater treatment process in two ways. Membranes in hollow fiber configuration can be added as a separate unit operation downstream of the biological step or membranes can be integrated into biological step as a membrane bioreactor (MBR) [28]. The other membrane separation process used in wastewater treatment is reverse osmosis (RO) which removes ions and organic matter [29]. However, it is being replaced by nanofiltration due to its lower energy consumption and higher flux rates [30]. Recently there is also an increasing interest in membrane distillation (MD) as an excellent potential for wastewater treatment as it does not require high pressure or addition of chemicals [31].

The water filtration market is still highly dominated by polymeric membranes due to their good permeability and selectivity and low production cost. However, the interest in ceramic membranes is increasing due to their many advantages over polymeric membranes [32]. Their high mechanical, chemical and thermal resistance, long lifespan and lower fouling tendency compared to polymeric membranes allow to use them in the harsh environment under wider pH (1-14) and high-pressure ranges [33],[34]. Nevertheless, ceramic membranes have some limitations to overcome such as low perm-selectivity and filtering area density and high production costs due to high price of raw materials and complex manufacturing [32],[35],[36],[37],[38]. At the

same time, membrane fouling is one of the most critical issues for the development of membrane processes [39]. Fouling is caused by the deposition of material on or within the structure of membranes, which leads to blockage of the membrane pores. It is characterized by the decrease of permeate flux or increase of the transmembrane pressure. Different fouling mechanisms such as pore blocking, cake formation, concentration polarization, biological fouling appear depending on the specific process [27]. Fouling can be irreversible if the dissolved matter is adsorbed in the pores or onto the membrane surface. This kind of fouling can be removed by chemical cleaning. Other methods, such as backwashing, pre-treatment of the feed or membrane modification can be also used to prevent fouling. In wastewater filtration, fouling is caused by organic matter compounds mainly natural organic matter, humic acids, dyes, surfactants, oils and phenolic compounds [39].

CHAPTER 2. THERMOCATALYTIC CERIUM-DOPED STRONTIUM FERRATE PEROVSKITE

Perovskites ceramic-type mixed metal oxide materials have the general formula ABO_3. Larger A-site cations (alkaline or rare earth metals) are located on the corners of the lattice and have 12-fold coordination with oxygen (O). The smaller B-site cations are 6-fold coordinated transition metals [40]. The image of the cubic perovskite structure as calculated by Rietveld refinement of the diffraction data is showed in Figure 8 [41].

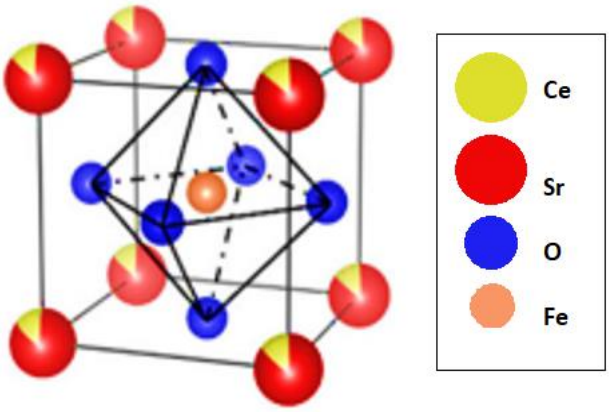

Figure 8. The image of the cubic perovskite structure. The iron octahedral site of the $Sr_{0.85}Ce_{0.15}FeO_{3-\delta}$ perovskite is highlighted, whereas the orange, red, yellow, and blue spheres indicate iron, strontium, cerium, and oxygen atoms, respectively. The figure is from Paper I.

In principle, it is possible to replace the A/B site cations by 90% of the metal elements in the periodic table without destroying the matrix crystal structure [42]. However, due to the fluctuation of the radius of cations, the crystal structure can deviate from the ideal form within a certain extent [19].

Perovskites are mainly synthesized by combustion, co-precipitation, sol-gel, and chelating precursor method. In this project, thermocatalytic cerium-doped strontium ferrate perovskite (CSF) was synthesized by solution-combustion synthesis (SCS) that is a fast and self-sustained redox reaction occurring between an oxidant (metal precursor) and a fuel (organic material) in presence of metal cations. The fuel is here citric acid, which have also the ability to form coordination complexes with the metal ions of interest. It should have a role of chelating agent and microstructural template. During combustion, the fuel is oxidized to gaseous products by the oxidants. At the

same time the metal cations are converted to oxides by taking the oxygen from the oxidant molecules [43]. The chemical reaction of CSF synthesis occurs as follows:

$$0.85\ Sr(NO_3)_2 + Fe(NO_3)_3 \cdot 9H_2O + 0.15\ Ce(NO_3)_3 \cdot 6H_2O + 11.56\ NH_4NO_3 + 4\ C_6H_8O_7 \rightarrow Sr_{0.85}Ce_{0.15}FeO_{3-\sigma} + x\ N_2 + y\ CO_2 + z\ H_2O \quad (3)$$

Where NH_4NO_3 is the additional oxidant and $C_6H_8O_7$ is the fuel.

Solution combustion synthesis is an excellent method for the synthesis of perovskites, due to its simplicity, high efficiency and high purity of produced powder, with well-defined properties such as higher surface area and narrow particle size distribution. SCS consists of four steps such as formation of combustion mixture, formation of the gel, combustion of the gel and formation of as-burned powder. The process is presented in Figure 9.

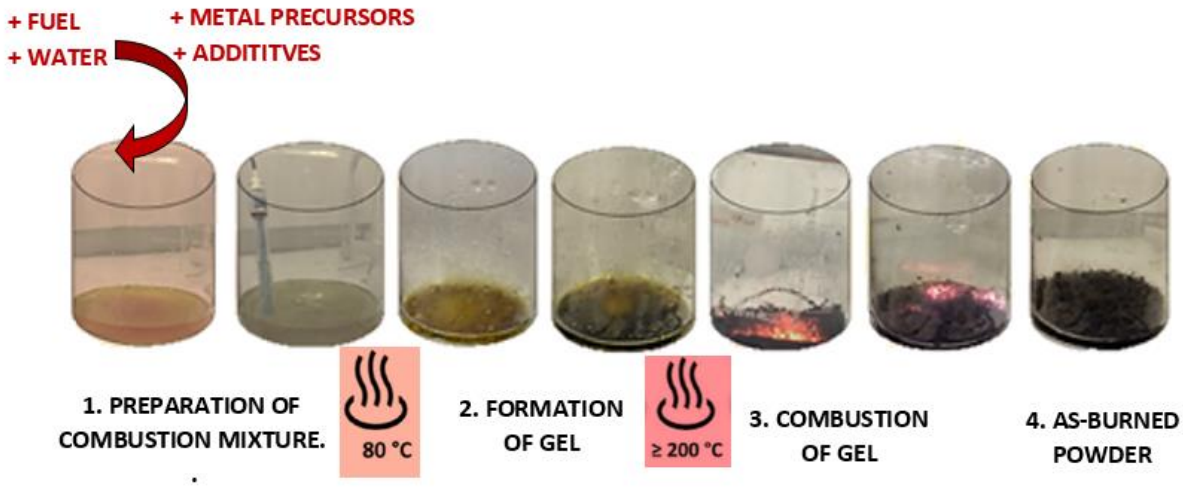

Figure 9. Solution combustion synthesis of cerium-doped strontium ferrate perovskite. As-burned powder was calcined in 1000 ºC for 5 h with heating rate 5 ºC/min.

Reducers-to oxidizers ratio φ was set to 1 in order to ensure stoichiometric ration with balanced reducing and oxidizing species. The redox-active cubic structure of strontium ferrate can be stabilized by cerium-doping.

2.1. REACTION MECHANISM OF THERMOCATALYTIC DEGRADATION OF ORGANIC POLLUTANTS BY PEROVSKITES

The reaction mechanism of thermocatalytic degradation of organic pollutants is not fully understand yet. Based on studies of Chen et al. the single-electron transfer (SET) that takes place between oxidant and the transition metal is the most possible mechanism (Figure 11 A) of the oxidation of the organic pollutants by perovskites in the darkness. The perovskite activates the oxidant to form reactive oxygen species (ROS), which are able to further react with the dissolved organic matter. The mechanism of peroxide activation on perovskite catalysts is presented in figure 10. During the activation process the low-valence transition metals M^{n+} first donates one electron and then they oxidize themselves to a high-valence state $M^{(n+1)+}$. The oxidants such as H_2O_2, HSO^{5-} and $S_2O_8^{2-}$ receive this electron and the dominant free radicals such as $^{\bullet}OH$ and $SO_4^{\bullet -}$ are formed as follows [19]:

$$M^{n+} + HSO_5^- \rightarrow M^{(n+1)+} + SO_4^{\bullet -} + OH^- \quad (4)$$

$$M^{n+} + H_2O_2 \rightarrow M^{(n+1)+} + \bullet OH + OH^- \quad (5)$$

$$M^{n+} + S_2O_8^{2-} \rightarrow M^{(n+1)} + SO_4^{\bullet -} + SO_4^{2-} \quad (6)$$

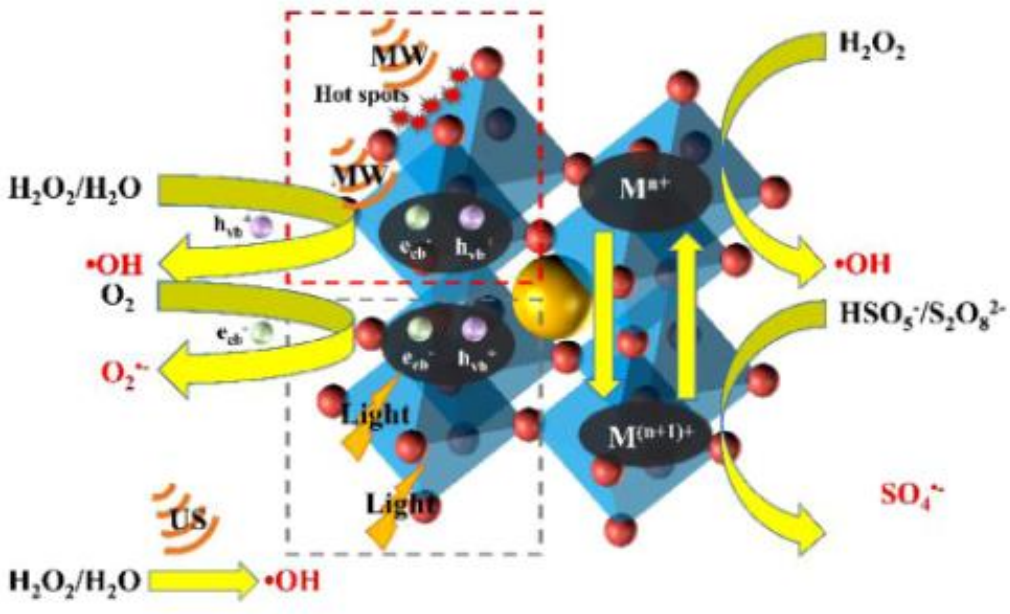

Figure 10. Possible mechanism of the activation of peroxides on perovskites, where MW = microwave activation and US = ultrasound, reprinted from [19].

Hopping conduction (HC) mechanism (Figure 11 B) is another possibility of degradation of organic pollutants. The mechanism occurs when the energy which is transferred to the catalyst equals or exceeds the catalyst band gap energy. It excites the electrons in the valence band (VB) into the conduction band (CB), leaving at the same time positive electron-holes (h^+) in the VB. These electron-holes have an oxidation potential which allows to directly oxidize H_2O_2 to hydroxyl radicals. At the same time electrons can be trapped by adsorbed oxygen creating ROS, which attack organic molecules. Some of excited electrons recombine with holes and dissipate the energy in either radiative or non-radiative ways. The mechanism can be described as follows:

$$\text{catalyst} + \text{heat excitation} \rightarrow \text{catalyst}\ (h^+ + e^-) \quad (7)$$

$$h^+ + H_2O \rightarrow {}^{\bullet}OH + H^+ \quad (8)$$

$$h^+ + e^- \rightarrow \text{energy} \quad (9)$$

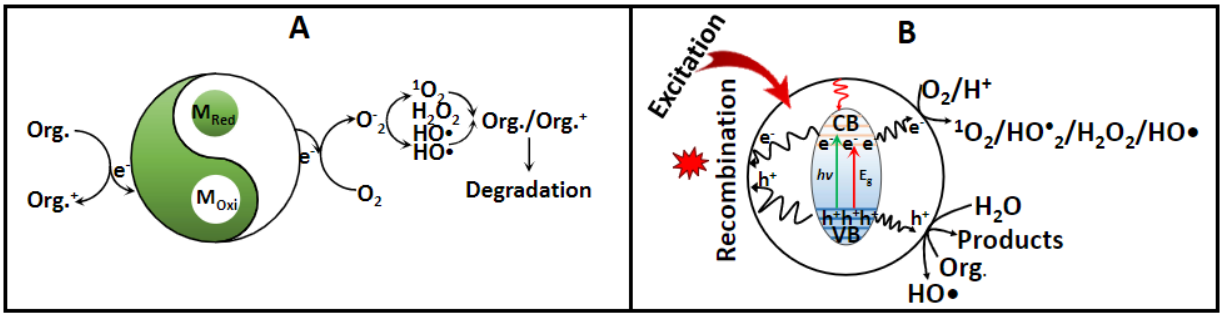

Figure 11. A – surface electron transfer mechanism (SET) and B - the hopping conduction mechanism of pollutants degradation, reprinted from [42].

2.2. BISPHENOL A ABATEMENT

Bisphenol A (2,2-bis-4-hydroxyphenylpropane, BPA) is an endocrine disrupting compound (EDC) that change and disturb the function of the endocrine system having serious effect on natural environment and individual health [44]. The BPA market for production of polycarbonate plastics and epoxy resins has been count for 6,000 kilotons in 2021. Due to its toxicity and high presence in environment, BPA has been classified as contaminant of emerging concern. Unfortunately, biological wastewater treatments are not effective in removal of BPA due to its ability to be absorbed on biofilm or suspended solids, which remain of high concentration after short sedimentation time during sludge granulation. Therefore, there is a need of post-treatment in order to reduce the concentration of BPA in the effluent and limit its harmful effects on environment [34]. Membranes are especially promising in BPA removal, since NF, RO and MD systems can reject also small organic molecules [45].

2.2.1. RELATION BETWEEN KINETIC RATE CONSTANT, CATALYST CONCENTRATION AND REACTION TEMPERATURE

It has been proved by many studies [46]–[50] that the reaction temperature has a significant effect on the degradation kinetics. The oxidation activation and pollutants degradation are higher with the increase of temperature. The increase of temperature causes increase of diffusion and adsorption rate of contaminants and at the same time it provides more energy for the cleavage O-O bonds causing formation of ROS. Based on the good fitting result of experimental data it has been found that Arrhenius equation can be used to correlate the degradation kinetics with temperature by predicting the rate constant *k* at different temperatures. The degradation rate constant increases with increasing temperature as follows [19].

$$k = A\ exp\left(-\frac{E_a}{RT}\right) \tag{10}$$

Where E_a is apparent activation energy of degradation (J mol^{-1}), A is the frequency constant (min^{-1}), R is the universal gas constant (J K^{-1} mol^{-1}), and T is the absolute temperature (K)

In Paper I we investigated the ability of CSF to degrade BPA in temperature range 30-60 ^oC and for CSF concentrations 0.15, 0.35 and 1.0 g L^{-1}. Reaction rates were calculated from concentration change over time and was plotted against BPA and perovskite concentrations.

The rate of BPA degradation has been determined from the equation:

$$r_{BPA} = kC_{BPA} \tag{11}$$

Where C_{BPA} is the BPA concentration.

In respect to BPA and perovskite concentrations, the rate of BPA degradation process was found to follow a pseudo first-order kinetic. It can be seen in Figure 12 that CSF was performing high activity in the degradation of BPA reaching the highest kinetic rate at 65 ^oC. The degradation rate was higher at higher temperatures.

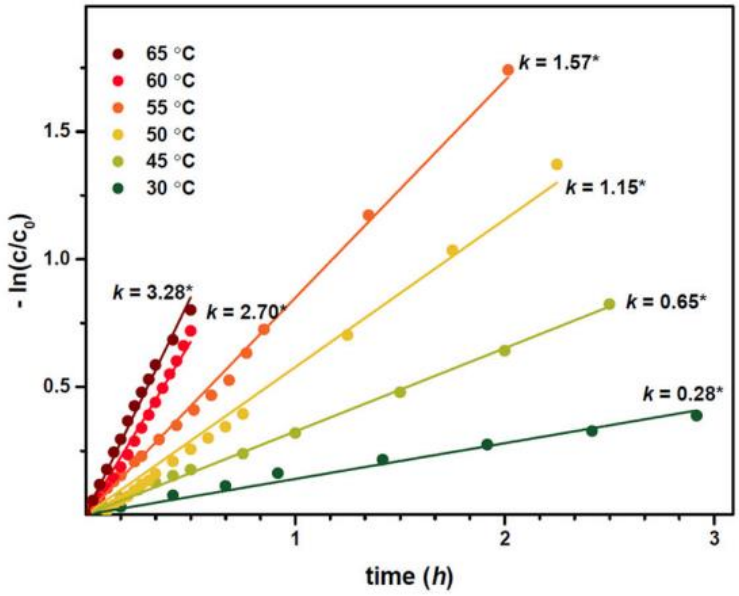

Figure 12. Influence of temperature on the degradation of BPA by CSF and correspondent rate constants, k (L g^{-1} h^{-1}) (where BPA initial concentration c_0 = 10 mg L^{-1}, CSF concentration c= 0.50 g L^{-1}). The figure is from Paper I.

The specific rate constants have been plotted as a function of the temperature in Figure 13 and they are consistent with the results of Leiw et al. who calculated the cubic CSF kinetic rate constant of 0.13 L g^{-1} h^{-1} at room temperature [51].

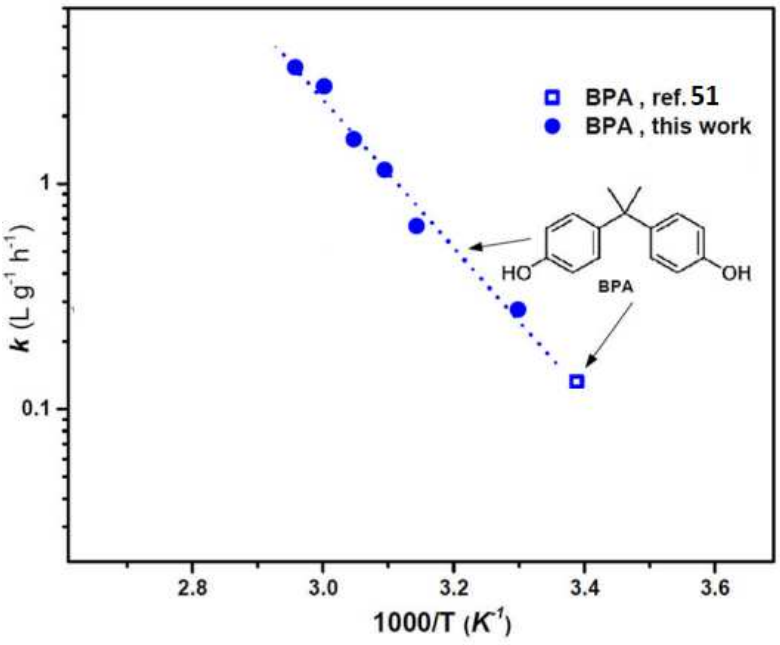

Figure 13. Temperature-dependence of kinetic constants for the abatement of BPA by cubic strontium ferrates. Figure is modified from Paper I.

2.2.2. THE IMPACT OF CATALYST LOADING ON THE BISPHENOL A ABATEMENT

We studied the model investigating the impact of CSF loading (0, 9, 18, 54, 90, 180 mg) on the BPA abatement by thermocatalytic membrane distillation (MD). It can be observed on Figure 14 that with no addition of CSF catalyst the pollutant is concentrated during filtration. While addition of 180 mg of CSF led to > 99% degradation of BPA and production of 1 L of distilled water.

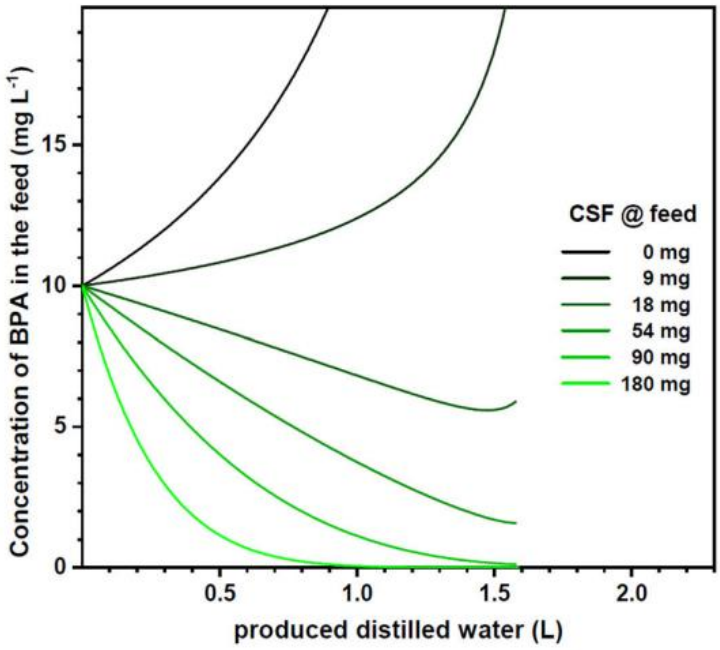

Figure 14. BPA concentration in the feed as a function of the produced distilled water for different CSF loadings (feed initial volume: 1.80 L, cross-flow velocity: 0.047 m s^{-1}, and temperatures in the feed and permeate beakers: 65 and 15 °C, respectively). The The figure is from Paper I.

We also investigated the impact of different CSF loading (1, 2 and 10 g L^{-1}) on BPA abatement (c_0=10 mg L^{-1}) in the combination with nanofiltration (NF) membrane (Figure 15). After 5 times concentration of effluent by NF, 50 mL samples of the concentrate were treated at 50 ◦C with CSF over 5 h. The results show that BPA abatement increases following the CSF concentration. At the same time, it demonstrates less efficiency of thermocatalyst in BPA abatement in real matrixes

which are richer in dissolved organic matter content than when the tests were performed with model solutions of contaminant in deionized water.

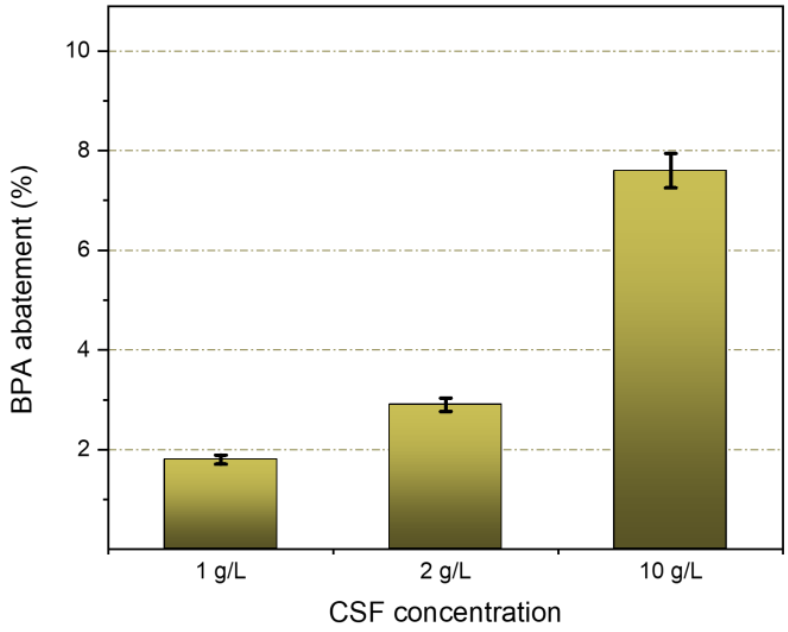

Figure 15. Abatement of BPA in the concentrated wastewater effluent after treatment with different amounts of CSF for 5 h. The The figure is from Paper II.

2.3. DEGRADATION OF NON-TOXIC ORGANIC MATTER

Wastewater streams often require further treatment before reuse, due to presence of many compounds such as natural organic matter (NOM), trace harmful chemicals and soluble microbial products (SMPs) [52].

The concentration of non-toxic dissolved organic matter in the wastewaters is much higher than the concentration of CECs and therefore it has a negative effect on both water permeance of the membrane and the thermocatalytic performances of degradation of pollutants by catalyst [53].

In this study, we showed that CSF can degrade part of the dissolved organic matter. The degradation of non-toxic organic matter by treatment with CSF thermocatalyst in a batch reactor is presented in Figure 16. It shows 35% abatement of COD after 5 h of treatment. However, it can be also seen that the overall COD abatement does not change significantly by increasing CSF concentration from 1.0 to 10 g L^{-1}. It can be explained by different types of chemical species present in dissolved organic matter from which some are highly recalcitrant to degradation, for example humic substances.

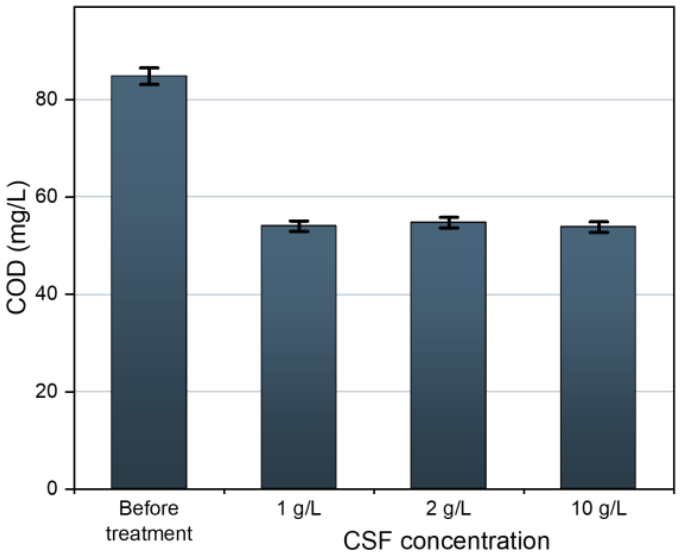

Figure 16. Concentration of COD in wastewater effluent before and after treatment with different CSF concentrations for 5 h. The figure is from Paper II.

NOM may present a negative influence on the filtration process causing clogging of the pores of membranes at the detriment of the membrane permeance. However, the ability of thermocatalyst to degrade non-toxic organic matter, helps to reduce the chemical oxygen demand of the retentate and at the same time decrease the fouling of membrane during filtration process.

In other study (Figure 17) we investigated the degradation of organic matter content by combined microfiltration with ozone and perovskite, for which COD removal efficiency of 44% was almost two times higher than for filtration with MF membrane (23.43%) and filtration with ozone (17.41%).

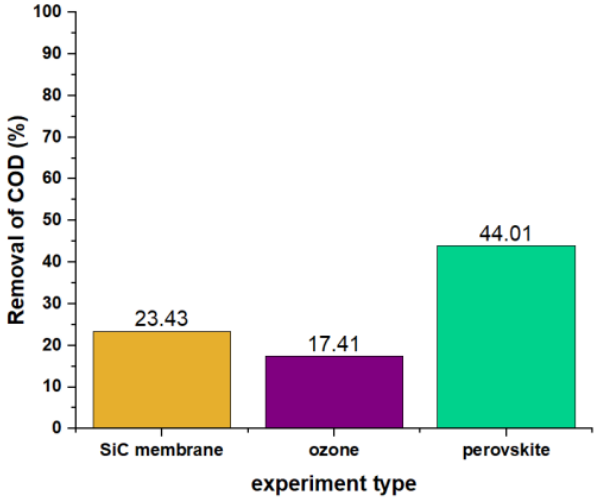

Figure 17. COD removal efficiency for different types of membranes. The figure is from Paper III.

CHAPTER 3. INTEGRATED MEMBRANE FILTRATION-THERMOCATALYTIC PROCESSES

3.1. MICROFILTRATION – SILICON CARBIDE MEMBRANE

Microfiltration (MF) is a low pressure-driven type of filtration. MF membranes have pore sizes between 0.1 and 10 μm and are used to concentrate, purify or separate suspended particles, colloids and macromolecules from solution. MF is usually operated in a cross-flow configuration.

Porous silicon carbide (SiC) membrane is one of the materials used for the fabrication of commercial Mf membranes. Commercially available SiC 30-channeled tubular membrane of porosity 40% obtained from Liqtech Ceramics A/S (Figure 18) was used for our experiments. This ceramic membrane of honeycomb structure shows high potential in wastewater treatment, due to its unique properties such as high mechanical strength, good chemical and thermal resistance, high thermal conductivity, and high hydrothermal stability. Moreover, it is stable in harsh environments, as in presence of high temperatures and strong chemicals [54][55].

Figure 18. Silicon carbide multi-channeled membrane from Liqtech Ceramics A/S.

The general role of microfiltration membrane is to purify the wastewater by reducing COD and turbidity reduction. Figure 19 shows the change of relative concentration of CECs (BPA, ibuprofen and caffeine) in the feed and permeate as a function of the filtration time over the SiC membrane. There is no significant difference between concentrations of pollutants in feed and permeate, what can be explained by large size of microfiltration membrane pores, which are too large to retain pollutants. The

decline in initial concentration of pollutants is observed, what can be explained by adsorption to suspended matter.

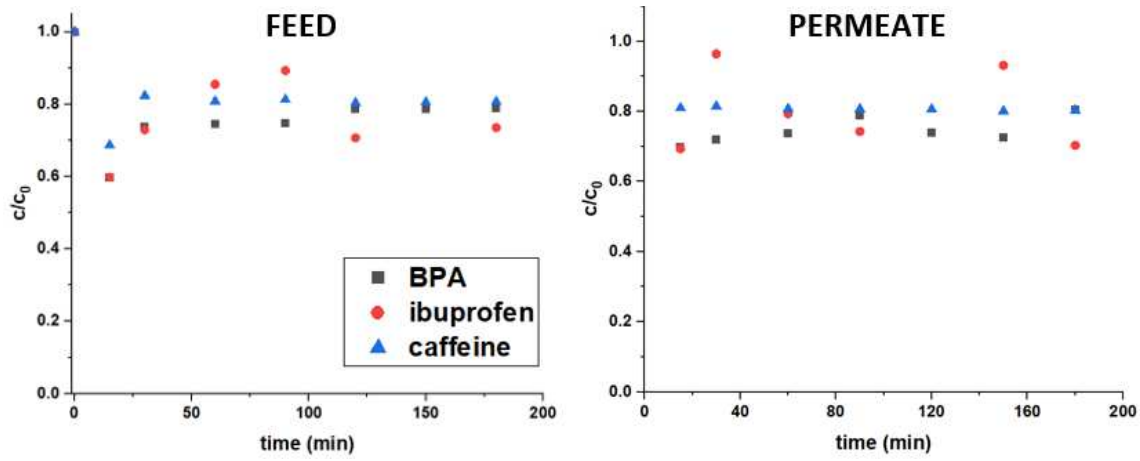

Figure 19. Change of relative concentration of CECs in time in feed and permeate for filtration with SiC membrane. The figure is from Paper III.

In this project, microfiltration was combined with AOP by thermocatalysis and ozonation in order to test the synergy between these processes. The comparison of the percentage removal of contaminants during 4 types of experiments is presented in Figure 20. As expected, the filtration with SiC membrane shows the lowest removal of contaminants while filtration with ozone and perovskite represents the highest removal of contaminants. Considering the degradation of BPA, the lowest removal of 19.52% was observed for filtration with SiC membrane, while the highest removal of 68.95% was observed for combination of filtration with ozone

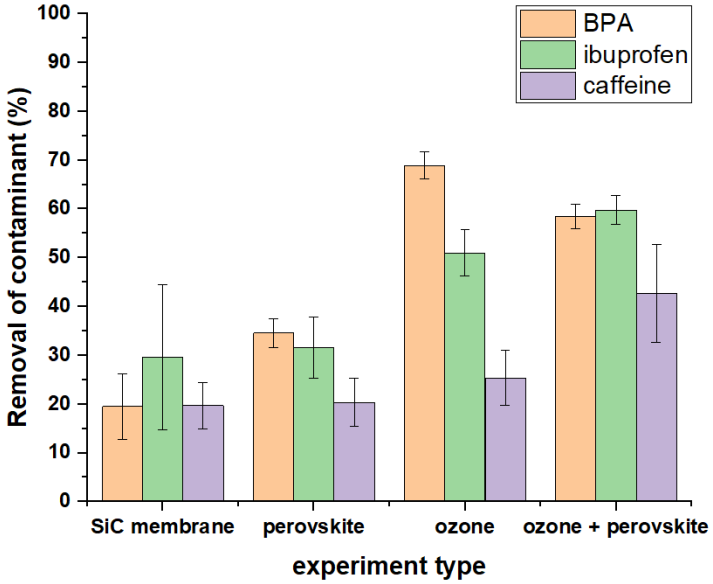

Figure 20. The removal of contaminants (%) in different types of experiments. The figure is from Paper III.

It was also found that during the microfiltration the membrane purifies the wastewater by reducing its turbidity. The rate of turbidity was calculated as the difference between the turbidity of permeate and the turbidity of initial feed before treatment. Figure 21 shows that the turbidity removal increase from 77% up to 89% for ozone. The clarity of treated water is also improved to 94% for filtration with perovskite and it reaches 97% for filtration with ozone and perovskite. The highest turbidity removal for experiments with perovskite can be a reason of perovskite ability of degradation of organic matter [56]. For experiments with ozone it can be explained by the coagulation or degradation of organic matter by the pre-ozonation [57].

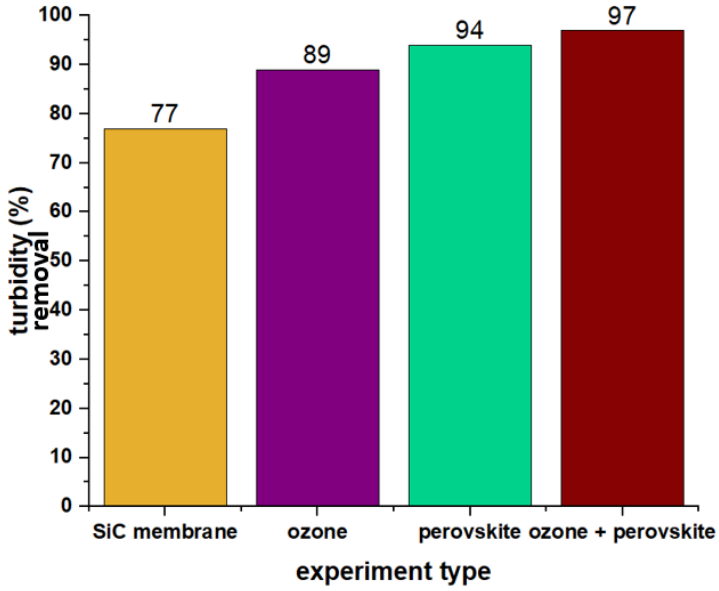

Figure 21. Turbidity removal (%) during different types of experiment. The figure is from Paper III.

3.2. NANOFILTRATION – ALUMINA-DOPED SILICA MEMBRANE

Nanofiltration (NF) membranes having pores of size 1-2 nm are sufficient for removal of multivalent salt ions and small organic pollutants. Alumina-doped silica amorphous membranes with narrow pore size and high pore volume and selectivity in the NF range have been recently developed at Aalborg University [58]. This tubular membrane is also characterized by high mechanical resistance, what allows to use it with thermocatalyst. However, the membrane is also distinguished by low stability in hydrothermal environment and basics solutions, what influence its permeability and selectivity. Therefore, the membrane was doped with metal oxides in order to increase

its stability and performances [58]. The Al_2O_3-doped silica membrane has been previously tested in different study showing good retention of organic CECs [58]. The idea of our experiments was to combine ceramic NF membrane with CSF perovskite for retention and degradation of Bisphenol A and for improvement of the quality of feed and permeate.

First, the impact of temperature on BPA rejection by NF membrane was studied, where the feed volume was 1.8 L and initial BPA concentration was 10 mg/L. Figure 22 shows that temperature has no impact on BPA rejection. Constant pollutant rejection can be observed for all tested temperatures 30 °C (98.7%), 40 °C (99.5%), 50 °C (98.6%), 55 °C (98.8%), 60 °C (98.9%)). Secondly, the impact of temperature on water permeance was checked. The cross flow was adjusted to value 1.6 ± 0.1 m s^{-1}, while the feed was pressurized at 6 bar. It can be seen in Figure 22 that the feed temperature has an influence on the water permeance. Indeed, the permeance increases by raising the temperature, reaching the value of 1.09 L (h m^2 bar)$^{-1}$ for 30 °C, 1.40 L (h m^2 bar)$^{-1}$ for 40 °C, 1.91 L (h m^2 bar)$^{-1}$ for 50 °C, 2.02 L(h m^2 bar)$^{-1}$ for 55 °C, and 2.17 L (h m^2 bar)$^{-1}$ for 60 °C. These values confirm literature results [59].

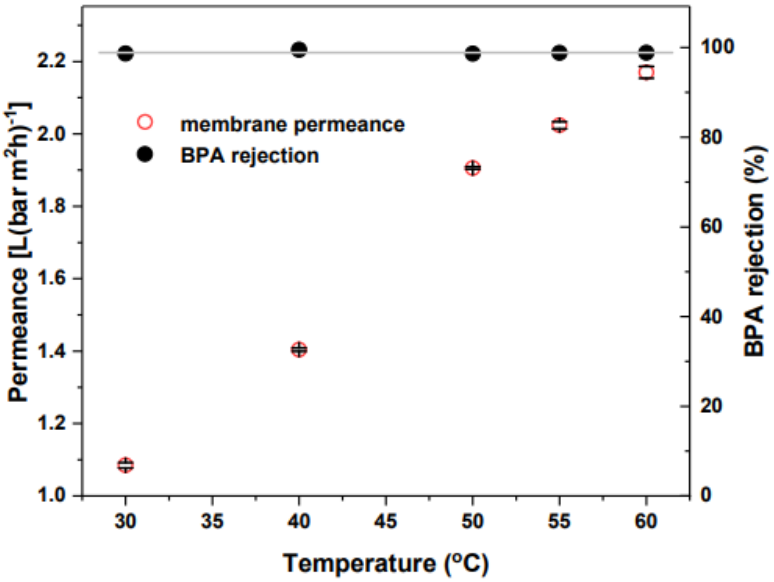

Figure 22. Impact of temperature on water permeance and BPA rejection for Al_2O_3 – doped silica membrane. The figure is from Paper II.

In order to study Bisphenol A abatement by perovskite the nanofiltration was performed at 50 °C with initial BPA concentration 10 mg/L. It can be observed that the BPA concentration in the feed (Figure 23a) remained stable for the first two hours of filtration and after adding the catalyst it significantly dropped until 4 g L^{-1} after 3 hours of experiment. The concentration of BPA in the permeate (Figure 23b), was stable during first 2 hours and oscillated around 0.19 mg/L. However slight increase was observed, what can be explained by the higher concentration at the retentate. In correspondence to significant decrease of concentration after adding the catalyst to the feed, the drop was observed as well in the permeate reaching value of 0.1 mg L^{-1} after 3 hours of experiment.

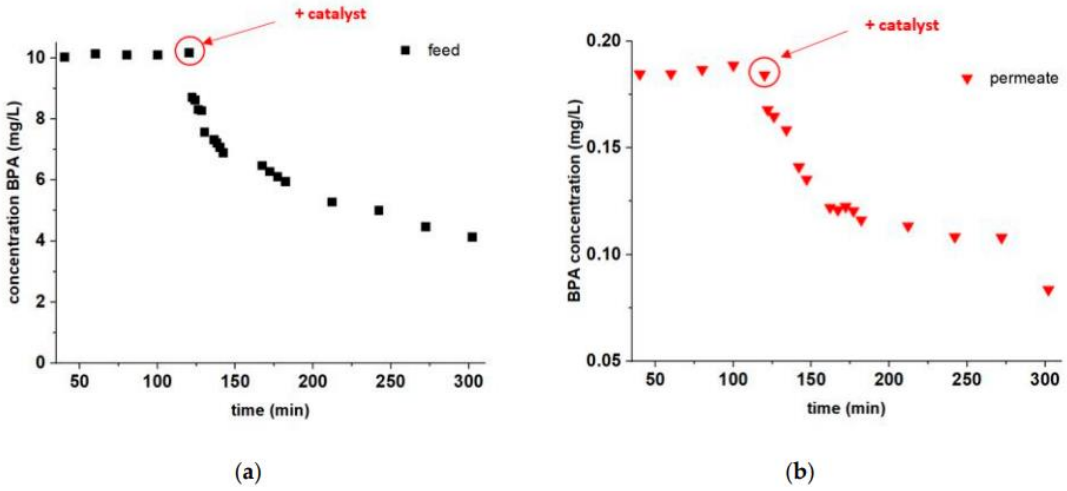

Figure 23. Thermocatalytic degradation of BPA concentration in the feed (a) and permeate (b) as a function of the filtration time. The figure is from Paper II.

3.3. MEMBRANE DISTILLATION – HOLLOW FIBERS MEMBRANE

Membrane distillation is a type of filtration with hydrophobic porous membrane produced from polymer materials such as polypropylene (PP), polytetrafluoroethylene (PTFE) and polyvinylidene fluoride (PVDF). The membrane is a physical barrier separating the hot feed from the permeate stream. At the same time the vapor pressure gradient is a driving force to pass volatile compounds from feed to permeate side. In order to produce the vapor MD works at relatively low temperatures which are under feed boiling point. In recent years membrane distillation (MD) has gained attention as a promising method to remove CECs from wastewater and produce clean water [61][62].

The module in Figure 24 consists of many polymeric hollow fibers built together to achieve high filtering area density. This module was used for membrane distillation (MD) is a in this study.

Combination of membrane filtration with thermocatalyst proposed in this study allows to draw of clean water at the permeate side of membrane (cold) and to degrade CECs concentrated at the feed side (hot) of membrane. The role of thermal energy is to drive water permeation through the membrane while activating generation of ROS by catalyst in order to degrade CECs. The membrane speeds up the degradation process by concentrating the pollutant during filtration process The integration of MD with thermocatalysis allows to obtain high purity distilled water from previously contaminated water and at the same time to reduce toxicity of CECs in the concentrate

stream. Moreover, this technology consists of simple process design and there is no need of additional chemicals or high pressure. The process is simple as the heat drives both permeation of distilled water and degradation of the pollutants by thermocatalyst through the membrane. It is also possible to save energy costs by using alternative heating sources, such as solar, geothermal, or low-grade waste heat from process streams.

Figure 24. Membrane distillation module of 40 polypropylene hollow fibers. The figure is from Paper I.

The hollow-fiber mode can be operated in two different ways. One of them is the inside-out mode (Figure 25A) in which the solution of feed passes through the bore of the fiber and the collection of permeate takes place on the outside side of the fiber. The other one is outside-in mode (Figure 25B) in which the entrance for the feed solutions is on the shell side of the fibers, while the permeate just passes into the fiber bore [60]. In this study the module was operated in the outside-in mode to avoid the clogging of the fibers by the thermocatalytic powder.

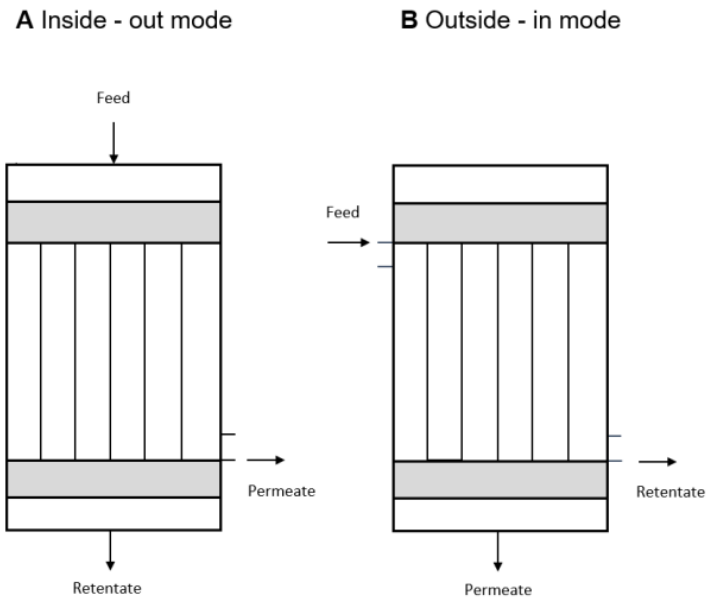

Figure 25. Modes to operate and hollow-fiber membrane module (A – inside-out mode, B – outside-in mode).

In this study the feed water spiked by BPA was heated at temperatures in the range between 30 and 65 °C to induce the degradation process by catalysys and at the same time to drive steam through a hollow fiber MD membrane. The tests were performed in direct contact MD module that works as a function either by pumping the feed on the shell side and the permeate inside the hollow fibers or opposite. In this case the feed was flowing at the shell side due to problems with clogging the fibers by perovskite after few hours of experiment.

From Figure 26, it can be seen the time required to reach 99% abatement of BPA at different temperatures of feed in the range 30 - 65 °C, assuming that the area of the MD could be varied from 0-1.5 m^2. Figure shows that 1.80 g of CSF is necessary to achieve >99% pollutant degradation while producing 1.0 L of clean water. The graph proves that there is a positive influence of larger membrane area on reduction of the abatement time, what is explained by the membrane concentrating the pollutant during its abatement. Therefore, the positive effect of the membrane is more obvious at lower temperatures, where the degradation rates are slower.

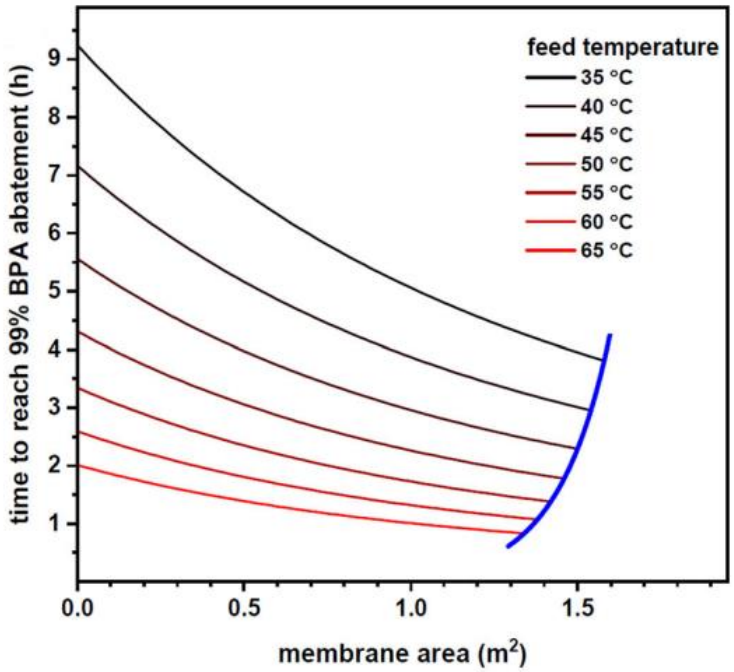

Figure 26. Relation between time needed to reach 99% degradation of BPA and membrane area at different feed temperatures. The initial C_{BPA}: 10 mg/L, CSF loading: 1.80 g. The figure is from Paper I.

Moreover, based on our experiment and simulation CSF can be reused up to 4 times. Catalyst was added to the feed at the beginning of first run. It can be seen from figure 27 that the experimental data in the 3rd and 4th runs corresponds well to the model (green lines). However, the degradation rates are faster than predicted for 1st and 2nd run, what can be explained by dispersion of catalyst powder inside the beaker with feed and migration of powder inside the MD module.

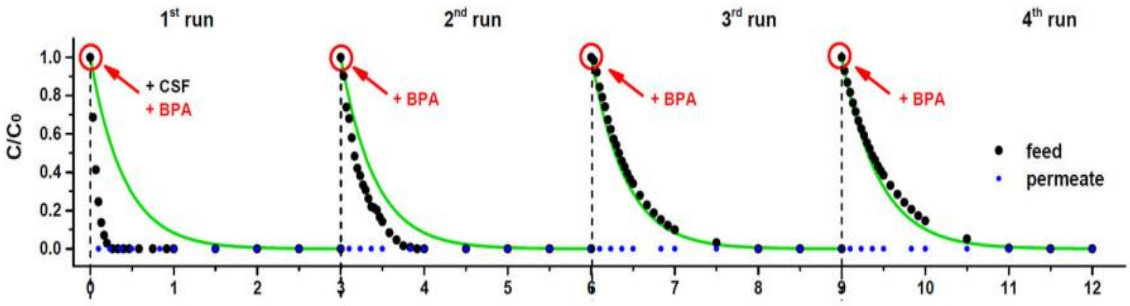

Figure 27. Change of relative concentration of BPA as a function of time during four consecutive runs of thermocatalytic distillation based on the simulation, where green line – simulation, dots – experimental points. The figure is from Paper I.

CHAPTER 4. CHALLENGES AND POTENIAL APPLICATIONS

New hybrid NF-thermocatalysis waster purification systems were presented in this thesis. Considering membranes, there are mostly cost related limitations to overcome. For SiC microfiltration membranes these are high costs of fabrication, processing, and the precursors. Another limitation of SiC membrane is their multistage preparation procedure. Some solutions for these problems have been proposed by Eray et al. [54] who suggest the reduction of costs by use of cheaper and more sustainable materials and by preparation of more efficient and simpler protocols of fabrication of SiC membrane. Also costs of MD modules are quite high due to the requirement of huge amount of thermal energy necessary to heat and keep the water temperature at the feed side. It makes the process economically profitable only in the presence of cheap heating sources.

There are also some challenges to overcome in aspect of thermocatalyst. One of them is the decreasing efficiency of catalytic activity of CSF perovskite over time caused by formation of poising carbonates on its surface. Carbonates are causing blockage of active sites of catalyst and its deactivation. The problem was investigated by Østergaard et al. [40] who studied the formation of carbonates in deionized water, in the air and during degradation of BPA by CSF catalyst. Based on this research, it was found that the perovskite catalyst that contains transition metals has less tendency to form carbonates than the one containing alkaline earth metal oxides. Moreover, the reversibility of carbonate formation was investigated by treatment of carbonated CSF catalyst at temperature 900 ^{o}C in the air for duration of 1 hour. It caused regeneration of catalyst and giving possibility for active sites for further reactions.

The high running costs are also an issue for the thermocatalytic step, which requires 1.167 kWh $(m^3 \circ C)^{-1}$ for heating wastewater [56]. Indeed, the wastewater stream should be heated to the temperature appropriate for the activation of catalyst (e.g., 50 ^{o}C) [63]. Nevertheless, low-great heat, such as waste-heat from industrial processes, and solar or geothermal energy sources can be used for heating the system, making the process convenient for implementation.

Another challenge is the upscaling of the process. The experiments performed in the laboratory scale were designed for CSF synthesis in few grams batches by solution combustion. The solutions for upsacaling the process were investigated by Deganello et al. who have suggested some strategies for large-scale synthesis of perovskites [43] and its industrial production.

Another aspect to consider is recovery and reusability of CSF. In this study, we proved reusability of CSF up to four thermocatalytic distillation runs. and the possible

implementation has to be conducted. The idea is to immobilize the catalyst in a fixed bed reactor for the process of organic pollutants abatement from wastewater effluent which should take place after the process of pre-concentration over a NF membrane.

The thermocatalytic NF process and CSF parameters should be also optimized according to the presence of non-toxic organic matter in real wastewater systems. Indeed, high concentrations of organic matter present in wastewater have negative effect on performance of CSF catalyst in abatement of contaminants, because it can adsorb on the catalyst active sites and act as a ROS scavenger. Moreover, it can foul the membrane reducing its water permeance [53].

Considering the experiments with integration of microfiltration with perovskite and ozone, the dosage of ozone applied to the effluent should be estimated, as well as the way to identify and remove the ozonation toxic by-products created from matrix components and CECs. The formation of transformation products has been investigated by Bourgin et al. [64] and Gulde et al. [65]. The by-products can be removed using granular activated carbon [66].

For membrane distillation the idea is to optimizate a new process, by combination of MD modules with a fixed-bed thermocatalytic reactor and test it with real water systems [42] [51] [67].

CHAPTER 5. CONCLUSIONS

The present thesis has focused on the integration of microfiltration, nanofiltration and membrane distillation with thermocatalyst, cerium-doped strontium ferrate perovskite, for the purification of wastewater.

Due to growing water demand it is of high importance to find a proper method for reusing wastewater. This method should degrade harmful for natural environment contaminants of emerging concern, especially as the conventional wastewater treatment plants (WWTPs), biological, and physical methods offer limited abatement of organic pollutants.

Thermocatalysis, which is a representant of advanced oxidation processes, is characterized by the production of reactive oxygen species. The advantage of using AOP is the mineralization of organic pollutant, instead of their concentration in the retentate. Moreover, it is not necessary to use additional chemicals or light sources for thermocatalytic perovskites, what makes them competitive with other advanced oxidation processes in terms of saving of energy and operation simplicity.

Membrane filtration processes are recently considered as an attractive solution due to the production of high quality water and lower sensitivity to the variations of feed quality.

Due to their specific properties the synergistic integration of advanced oxidation and membrane filtration processes is especially beneficial as one method supplement the advantages and eliminate the limitations of the other.

The combination of microfiltration with thermocatalyst and ozone leads to higher clarification of treated wastewater and lower toxicity. The wastewater can be polished by silicon carbide membrane by simultaneous removal of turbidity, while ozone and cerium-doped strontium ferrate can help to degrade contaminants of emerging concern.

Integration of CSF with nanofiltration alumina doped silica membrane allows for abatement of organic pollutants, while at the same time it is mitigating membrane fouling and improving the permeate quality. The studies of pre-concentration of wastewater by NF allow to reduce the thermal energy required for the thermocatalytic process, as well as investment and running costs.

Addition of perovskite helped also to degrade non-toxic organic matter and reduce fouling. It also showed ability to reduce the COD of wastewater after pre-concentration by NF.

Membrane distillation requires much lower operating pressure than other filtration processes and lead to the production of pure water with no toxic concentrate. The

integration of MD with CSF shows advantages over batch catalysis such as faster degradation of pollutants and recovery of catalyst without additional steps.

To summarize, this work presents the new technology of wastewater streams treatment coupling highly stable and active thermocatalysis used for degradation of broad spectrum of CECs. membrane filtration units with high productivity of purified water and new design solutions for these integrated systems.

Bibliography

[1] S. Hube et al., "Direct membrane filtration for wastewater treatment and resource recovery: A review," Science of the Total Environment, vol. 710. Elsevier B.V., Mar. 25, 2020. doi: 10.1016/j.scitotenv.2019.136375.

[2] A. I. Shah, M. U. Din Dar, R. A. Bhat, J. P. Singh, K. Singh, and S. A. Bhat, "Prospectives and challenges of wastewater treatment technologies to combat contaminants of emerging concerns," Ecological Engineering, vol. 152. Elsevier B.V., Jun. 01, 2020. doi: 10.1016/j.ecoleng.2020.105882.

[3] H. Sousa, C. A. Sousa, L. C. Simões, and M. Simões, "Microalgal-based removal of contaminants of emerging concern," Journal of Hazardous Materials, vol. 423. Elsevier B.V., Feb. 05, 2022. doi: 10.1016/j.jhazmat.2021.127153.

[4] N. Bolong, A. F. Ismail, M. R. Salim, and T. Matsuura, "A review of the effects of emerging contaminants in wastewater and options for their removal," Desalination, 2009, doi: 10.1016/j.desal.2008.03.020.

[5] O. M. Rodriguez-Narvaez, J. M. Peralta-Hernandez, A. Goonetilleke, and E. R. Bandala, "Treatment technologies for emerging contaminants in water: A review," Chemical Engineering Journal. 2017. doi: 10.1016/j.cej.2017.04.106.

[6] V. Barbosa et al., "Effects of steaming on contaminants of emerging concern levels in seafood," Food and Chemical Toxicology, vol. 118, pp. 490–504, Aug. 2018, doi: 10.1016/j.fct.2018.05.047.

[7] B. Huidobro-López, I. López-Heras, C. Alonso-Alonso, V. Martínez-Hernández, L. Nozal, and I. de Bustamante, "Analytical method to monitor contaminants of emerging concern in water and soil samples from a non-conventional wastewater treatment system," J Chromatogr A, vol. 1671, May 2022, doi: 10.1016/j.chroma.2022.463006.

[8] W. Guo et al., "Retention of emerging CECs from UP water and a municipal secondary effluent by ultrafiltration and nanofiltration," J Memb Sci, vol. 287, no. 1, pp. 27–34, 2010, doi: 10.1016/j.memsci.2006.10.034.

[9] L. Rizzo et al., "Consolidated vs new advanced treatment methods for the removal of contaminants of emerging concern from urban wastewater," Science of the Total Environment, vol. 655. Elsevier B.V., pp. 986–1008, Mar. 10, 2019. doi: 10.1016/j.scitotenv.2018.11.265.

[10] P. Valbonesi, M. Profita, I. Vasumini, and E. Fabbri, “Contaminants of emerging concern in drinking water: Quality assessment by combining chemical and biological analysis,” Science of the Total Environment, vol. 758, Mar. 2021, doi: 10.1016/j.scitotenv.2020.143624.

[11] P. Singh, P. Shandilya, P. Raizada, A. Sudhaik, A. Rahmani-Sani, and A. Hosseini-Bandegharaei, “Review on various strategies for enhancing photocatalytic activity of graphene based nanocomposites for water purification,” Arabian Journal of Chemistry, vol. 13, no. 1. Elsevier B.V., pp. 3498–3520, Jan. 01, 2020. doi: 10.1016/j.arabjc.2018.12.001.

[12] M. Zielinska, I. Wojnowska-Baryla, and A. Cydzik-Kwiatkowska, Bisphenol A removal from water and wastewater. Springer, 2018. doi: 10.1007/978-3-319-92361-1.

[13] “Physicochemical Treatment Processes.”

[14] Y. Deng and R. Zhao, “Advanced Oxidation Processes (AOPs) in Wastewater Treatment,” Current Pollution Reports, vol. 1, no. 3. Springer, pp. 167–176, Sep. 01, 2015. doi: 10.1007/s40726-015-0015-z.

[15] J. M. Poyatos, M. M. Muñio, M. C. Almecija, J. C. Torres, E. Hontoria, and F. Osorio, “Advanced oxidation processes for wastewater treatment: State of the art,” Water Air Soil Pollut, vol. 205, no. 1–4, pp. 187–204, Jan. 2010, doi: 10.1007/s11270-009-0065-1.

[16] M. hui Zhang, H. Dong, L. Zhao, D. xi Wang, and D. Meng, “A review on Fenton process for organic wastewater treatment based on optimization perspective,” Science of the Total Environment, vol. 670. Elsevier B.V., pp. 110–121, Jun. 20, 2019. doi: 10.1016/j.scitotenv.2019.03.180.

[17] R. Andreozzi, “Advanced oxidation processes (AOP) for water purification and recovery,” Catal Today, 1999, doi: 10.1016/S0920-5861(99)00102-9.

[18] M. L. Rojas-Cervantes and E. Castillejos, “Perovskites as catalysts in advanced oxidation processes for wastewater treatment,” Catalysts, vol. 9, no. 3. MDPI, Mar. 01, 2019. doi: 10.3390/catal9030230.

[19] R. Ji, J. Chen, T. Liu, X. Zhou, and Y. Zhang, “Critical review of perovskites-based advanced oxidation processes for wastewater treatment: Operational parameters, reaction mechanisms, and prospects,” Chinese Chemical Letters, vol. 33, no. 2. Elsevier B.V., pp. 643–652, Feb. 01, 2022. doi: 10.1016/j.cclet.2021.07.043.

[20] J. Wang and H. Chen, “Catalytic ozonation for water and wastewater treatment: Recent advances and perspective,” Science of the Total

Environment, vol. 704. Elsevier B.V., Feb. 20, 2020. doi: 10.1016/j.scitotenv.2019.135249.

[21] J. L. Wang and L. J. Xu, "Advanced oxidation processes for wastewater treatment: Formation of hydroxyl radical and application," Crit Rev Environ Sci Technol, vol. 42, no. 3, pp. 251–325, Feb. 2012, doi: 10.1080/10643389.2010.507698.

[22] R. Dewil, D. Mantzavinos, I. Poulios, and M. A. Rodrigo, "New perspectives for Advanced Oxidation Processes," Journal of Environmental Management, vol. 195. Academic Press, pp. 93–99, Jun. 15, 2017. doi: 10.1016/j.jenvman.2017.04.010.

[23] H. T. Madsen, "Membrane Filtration in Water Treatment - Removal of CECs," in Chemistry of Advanced Environmental Purification Processes of Water: Fundamentals and Applications, Elsevier Inc., 2014, pp. 199–248. doi: 10.1016/B978-0-444-53178-0.00006-7.

[24] Z. Dai, L. Ansaloni, and L. Deng, "Recent advances in multi-layer composite polymeric membranes for CO2 separation: A review," Green Energy and Environment, vol. 1, no. 2. KeAi Publishing Communications Ltd., pp. 102–128, Jul. 01, 2016. doi: 10.1016/j.gee.2016.08.001.

[25] A. Karabelas and K. Plakas, "Membrane Treatment of Potable Water for Pesticides Removal," in Herbicides, Theory and Applications, InTech, 2011. doi: 10.5772/13240.

[26] "Cross Flow Filtration Method Handbook."

[27] M. A. Abd El-Ghaffar and H. A. Tieama, "A Review of Membranes Classifications, Configurations, Surface Modifications, Characteristics and Its Applications in Water Purification," Chemical and Biomolecular Engineering, vol. 2, no. 2, pp. 57–82, 2017, doi: 10.11648/j.cbe.20170202.11.

[28] S. Fazal, B. Zhang, Z. Zhong, L. Gao, and X. Chen, "Industrial Wastewater Treatment by Using MBR (Membrane Bioreactor) Review Study," J Environ Prot (Irvine, Calif), vol. 06, no. 06, pp. 584–598, 2015, doi: 10.4236/jep.2015.66053.

[29] E. Dialynas, D. Mantzavinos, and E. Diamadopoulos, "Advanced treatment of the reverse osmosis concentrate produced during reclamation of municipal wastewater," Water Res, vol. 42, no. 18, pp. 4603–4608, 2008, doi: 10.1016/j.watres.2008.08.008.

[30] H. K. Shon, S. Phuntsho, D. S. Chaudhary, S. Vigneswaran, and J. Cho, "Nanofiltration for water and wastewater treatment - A mini review," Drink

Water Eng Sci, vol. 6, no. 1, pp. 47–53, Jun. 2013, doi: 10.5194/dwes-6-47-2013.

[31] H. Julian, N. Nurgirisia, G. Qiu, Y. P. Ting, and I. G. Wenten, "Membrane distillation for wastewater treatment: Current trends, challenges and prospects of dense membrane distillation," Journal of Water Process Engineering, vol. 46, Apr. 2022, doi: 10.1016/j.jwpe.2022.102615.

[32] Z. He, Z. Lyu, Q. Gu, L. Zhang, and J. Wang, "Ceramic-based membranes for water and wastewater treatment," Colloids Surf A Physicochem Eng Asp, vol. 578, 2019, doi: 10.1016/j.colsurfa.2019.05.074.

[33] S. Benfer, U. Popp, H. Richter, C. Siewert, and G. Tomandl, "Development and characterization of ceramic nanofiltration membranes," Sep Purif Technol, vol. 22–23, pp. 231–237, 2001, doi: 10.1016/S1383-5866(00)00133-7.

[34] M. Zielińska, A. Cydzik-Kwiatkowska, K. Bułkowska, K. Bernat, and I. Wojnowska-Baryła, "Treatment of Bisphenol A-Containing Effluents from Aerobic Granular Sludge Reactors with the Use of Microfiltration and Ultrafiltration Ceramic Membranes," Water Air Soil Pollut, vol. 228, no. 8, 2017, doi: 10.1007/s11270-017-3450-1.

[35] X. Ma et al., "Surfactant-assisted fabrication of alumina-doped amorphous silica nanofiltration membranes with enhanced water purification performances," Nanomaterials, vol. 9, no. 10, pp. 1–12, 2019, doi: 10.3390/nano9101368.

[36] A. Farsi et al., "Design and fabrication of silica-based nanofiltration membranes for water desalination and detoxification," Microporous and Mesoporous Materials, vol. 237, pp. 117–126, 2017, doi: 10.1016/j.micromeso.2016.09.022.

[37] A. Farsi, S. H. Jensen, P. Roslev, V. Boffa, and M. L. Christensen, "Inorganic membranes for the recovery of effluent from municipal wastewater treatment plants," Ind Eng Chem Res, vol. 54, no. 13, pp. 3462–3472, 2015, doi: 10.1021/acs.iecr.5b00064.

[38] S. Mestre, A. Gozalbo, M. M. Lorente-Ayza, and E. Sánchez, "Low-cost ceramic membranes: A research opportunity for industrial application," J Eur Ceram Soc, vol. 39, no. 12, pp. 3392–3407, 2019, doi: 10.1016/j.jeurceramsoc.2019.03.054.

[39] F. E. Bortot Coelho, D. Deemter, V. M. Candelario, V. Boffa, S. Malato, and G. Magnacca, "Development of a photocatalytic zirconia-titania ultrafiltration

membrane with anti-fouling and self-cleaning properties," J Environ Chem Eng, vol. 9, no. 6, Dec. 2021, doi: 10.1016/j.jece.2021.106671.

[40] M. B. Østergaard, A. B. Strunck, V. Boffa, and M. K. Jørgensen, "Kinetics of Strontium Carbonate Formation on a Ce-Doped SrFeO3 Perovskite," Catalysts, vol. 12, no. 3, Mar. 2022, doi: 10.3390/catal12030265.

[41] M. B. Østergaard, A. B. Strunck, V. Boffa, and M. K. Jørgensen, "Kinetics of Strontium Carbonate Formation on a Ce-Doped SrFeO3 Perovskite," Catalysts, vol. 12, no. 3, Mar. 2022, doi: 10.3390/catal12030265.

[42] H. Chen, J. Ku, and L. Wang, "Thermal catalysis under dark ambient conditions in environmental remediation: Fundamental principles, development, and challenges," 2019. [Online]. Available: http://www.sciencedirect.com/science/journal/18722067

[43] F. Deganello and A. K. Tyagi, "Solution combustion synthesis, energy and environment: Best parameters for better materials," Progress in Crystal Growth and Characterization of Materials, vol. 64, no. 2, pp. 23–61, 2018, doi: 10.1016/j.pcrysgrow.2018.03.001.

[44] D. A. Juan, H. A. Hasan, M. H. Muhamad, S. R. S. Abdullah, S. N. H. A. Bakar, and J. Buhari, "Physico-chemical and Biological Techniques of Bisphenol A Removal in an Aqueous Solution," Journal of Ecological Engineering, vol. 22, no. 9, pp. 136–148, 2021, doi: 10.12911/22998993/141333.

[45] M. Zielińska, A. Cydzik-Kwiatkowska, K. Bułkowska, K. Bernat, and I. Wojnowska-Baryła, "Treatment of Bisphenol A-Containing Effluents from Aerobic Granular Sludge Reactors with the Use of Microfiltration and Ultrafiltration Ceramic Membranes," Water Air Soil Pollut, vol. 228, no. 8, 2017, doi: 10.1007/s11270-017-3450-1.

[46] K. Y. A. Lin and T. Y. Lin, "Degradation of Acid Azo Dyes Using Oxone Activated by Cobalt Titanate Perovskite," Water Air Soil Pollut, vol. 229, no. 1, Jan. 2018, doi: 10.1007/s11270-017-3648-2.

[47] S. Lu, G. Wang, S. Chen, H. Yu, F. Ye, and X. Quan, "Heterogeneous activation of peroxymonosulfate by LaCo1-xCuxO3 perovskites for degradation of organic pollutants," J Hazard Mater, vol. 353, pp. 401–409, Jul. 2018, doi: 10.1016/j.jhazmat.2018.04.021.

[48] K. Y. A. Lin, Y. C. Chen, and Y. F. Lin, "LaMO3 perovskites (M=Co, Cu, Fe and Ni) as heterogeneous catalysts for activating peroxymonosulfate in water," Chem Eng Sci, vol. 160, pp. 96–105, Mar. 2017, doi: 10.1016/j.ces.2016.11.017.

[49] S. ben Hammouda, F. Zhao, Z. Safaei, I. Babu, D. L. Ramasamy, and M. Sillanpää, “Reactivity of novel Ceria–Perovskite composites CeO2- LaMO3 (MCu, Fe) in the catalytic wet peroxidative oxidation of the new emergent pollutant ‘Bisphenol F’: Characterization, kinetic and mechanism studies,” Appl Catal B, vol. 218, pp. 119–136, 2017, doi: 10.1016/j.apcatb.2017.06.047.

[50] O. P. Taran, A. B. Ayusheev, O. L. Ogorodnikova, I. P. Prosvirin, L. A. Isupova, and V. N. Parmon, “Perovskite-like catalysts LaBO3 (B=Cu, Fe, Mn, Co, Ni) for wet peroxide oxidation of phenol,” Appl Catal B, vol. 180, pp. 86–93, Jan. 2016, doi: 10.1016/j.apcatb.2015.05.055.

[51] M. Y. Leiw, G. H. Guai, X. Wang, M. S. Tse, C. M. Ng, and O. K. Tan, “Dark ambient degradation of Bisphenol A and Acid Orange 8 as organic pollutants by perovskite SrFeO3-δmetal oxide,” J Hazard Mater, vol. 260, pp. 1–8, 2013, doi: 10.1016/j.jhazmat.2013.04.031.

[52] H. K. Shon, S. Vigneswaran, and S. A. Snyder, “Effluent organic matter (EfOM) in wastewater: Constituents, effects, and treatment,” Critical Reviews in Environmental Science and Technology, vol. 36, no. 4. pp. 327–374, Jul. 2006. doi: 10.1080/10643380600580011.

[53] I. Oller, S. Miralles-cuevas, A. Agüera, and S. Malato, “Monitoring and Removal of Organic Micro-pollutants by Combining Membrane Technologies with Advanced Oxidation Processes,” pp. 1–17, 2018, doi: 10.2174/1385272822666180404152113.

[54] E. Eray, V. Boffa, M. K. Jørgensen, G. Magnacca, and V. M. Candelario, “Enhanced fabrication of silicon carbide membranes for wastewater treatment: From laboratory to industrial scale,” J Memb Sci, vol. 606, Jul. 2020, doi: 10.1016/j.memsci.2020.118080.

[55] J. H. Eom, Y. W. Kim, and S. Raju, “Processing and properties of macroporous silicon carbide ceramics: A review,” Journal of Asian Ceramic Societies, vol. 1, no. 3. Taylor and Francis Ltd., pp. 220–242, 2013. doi: 10.1016/j.jascer.2013.07.003.

[56] K. Janowska, X. Ma, V. Boffa, M. K. Jørgensen, and V. M. Candelario, “membranes Combined Nanofiltration and Thermocatalysis for the Simultaneous Degradation of CECs, Fouling Mitigation and Water Purification,” 2021, doi: 10.3390/membranes.

[57] H. Cui, X. Huang, Z. Yu, P. Chen, and X. Cao, “Application progress of enhanced coagulation in water treatment,” RSC Adv, vol. 10, no. 34, pp. 20231–20244, May 2020, doi: 10.1039/d0ra02979c.

[58] X. Ma et al., “Surfactant-assisted fabrication of alumina-doped amorphous silica nanofiltration membranes with enhanced water purification performances,” Nanomaterials, vol. 9, no. 10, Oct. 2019, doi: 10.3390/nano9101368.

[59] T. Tsuru, S. Izumi, T. Yoshioka, and M. Asaeda, “Temperature Effect on Transport Performance by Inorganic Nanofiltration Membranes,” vol. 46, no. 3, 2000.

[60] “Advanced Physicochemical Treatment Processes.”

[61] M. Rahman Choudhury, N. Anwar, D. Jassby, and M. Saifur Rahaman, “Historical Perspective Fouling and wetting in the membrane distillation driven wastewater reclamation process-A review,” 2019.

[62] H. Julian, N. Nurgirisia, G. Qiu, Y. P. Ting, and I. G. Wenten, “Membrane distillation for wastewater treatment: Current trends, challenges and prospects of dense membrane distillation,” Journal of Water Process Engineering, vol. 46, Apr. 2022, doi: 10.1016/j.jwpe.2022.102615.

[63] Y. Zhang, T. Rottiers, B. Meesschaert, L. Pinoy, and B. van der Bruggen, Wastewater Treatment by Renewable Energy Driven Membrane Processes. Elsevier Inc., 2019. doi: 10.1016/b978-0-12-813545-7.00001-5.

[64] M. Bourgin et al., “Evaluation of a full-scale wastewater treatment plant upgraded with ozonation and biological post-treatments: Abatement of CECs, formation of transformation products and oxidation by-products,” Water Res, vol. 129, pp. 486–498, Feb. 2018, doi: 10.1016/j.watres.2017.10.036.

[65] R. Gulde, M. Rutsch, B. Clerc, J. E. Schollée, U. von Gunten, and C. S. McArdell, “Formation of transformation products during ozonation of secondary wastewater effluent and their fate in post-treatment: From laboratory- to full-scale,” Water Res, vol. 200, Jul. 2021, doi: 10.1016/j.watres.2021.117200.

[66] A. Papageorgiou, D. Voutsa, and N. Papadakis, “Occurrence and fate of ozonation by-products at a full-scale drinking water treatment plant,” Science of the Total Environment, vol. 481, no. 1, pp. 392–400, May 2014, doi: 10.1016/j.scitotenv.2014.02.069.

[67] L. D. Tijing, Y. Chul, J. Choi, S. Lee, S. Kim, and H. Kyong, “Fouling and its control in membrane distillation — A review,” J Memb Sci, vol. 475, pp. 215–244, 2015, doi: 10.1016/j.memsci.2014.09.042.

[68] K. Janowska et al., “Thermocatalytic membrane distillation for clean water production,” NPJ Clean Water, vol. 3, no. 1, pp. 1–7, 2020, doi: 10.1038/s41545-020-00082-2.

[69] S. Miralles-Cuevas, I. Oller, A. Agüera, J. A. S. Pérez, R. Sánchez-Moreno, and S. Malato, “Is the combination of nanofiltration membranes and AOPs for removing microcontaminants cost effective in real municipal wastewater effluents?,” Environ. Sci.: Water Res. Technol., vol. 2, no. 3, pp. 511–520, 2016, doi: 10.1039/C6EW00001K.

List of publications

1) L.I. Moran Ayala, M. Paquet, **K. Janowska**, Paul Jamard, Cejna A. Quist-Jensen, Gabriela N. Bosio, D. O. Mártire, D. Fabbri, V. Boffa, "Water Defluoridation: Nanofiltration vs Membrane Distillation". Industrial and Engineering Chemistry Research¸ 2018, 57, 43, 14740-14748.

2) X.Z. Ma, **K. Janowska**, V. Boffa, D. Fabbri, G. Magnacca, P. Calza, Y. Yue, "Surfactant-assisted Fabrication of Alumina-doped Amorphous Silica Nanofiltration Membranes with Enhanced Water Purification Performances". Nanomaterials 2019, 9, 1368.

3) **K. Janowska**, V. Boffa*, M.* Koustrup *Jørgensen,* C.A. Quist-Jensen, F. Hubac, F. Deganello, F. E. Bortot Coelho, G. Magnacca, "Thermocatalytic membrane distillation for clean water production", Nature Clean Water, 2020 3:34

4) **K.Janowska**, X.Z. Ma, V.Boffa, M. Koustrup Jørgensen, V. M. Candelario, "Combined Nanofiltration and Thermocatalysis for the Simultaneous Degradation of CECs", Fouling Mitigation and Water Purification, , Membranes 2021, *11*(8), 639

5) **K. Janowska**, M. Koustrup Jørgensen, E. Eray, V. M. Candelario, V. Boffa, "Integrating Ceramic Membrane Filtration with Ozonation and Thermocatalysis for Wastewater Purification", to be submitted to Chemical Engineering Journal Advances

Paper I

npj | Clean Water

www.nature.com/npjcleanwater

ARTICLE OPEN

Check for updates

Thermocatalytic membrane distillation for clean water production

Katarzyna Janowska[1], Vittorio Boffa[1]✉, Mads Koustrup Jørgensen[1], Cejna Anna Quist-Jensen[1], Fabien Hubac[1], Francesca Deganello[2], Fabrício E. Bortot Coelho[3] and Giuliana Magnacca[3,4]

Natural water bodies and treated wastewaters contain an increasing variety of organic micropollutants with a negative impact on ecosystems and human health. Herein, we propose an integrated process based on membrane distillation and advanced oxidation, in which thermal energy is simultaneously used to drive the permeation of pure water through a hydrophobic membrane and to activate the generation of reactive oxygen species by a thermocatalytic perovskite, namely Ce-doped strontium ferrate. At a feed temperature of 65 °C, our thermocatalytic distillation apparatus can effectively retain and degrade bisphenol A, as model pollutant, while producing distilled water at the constant rate of 1.60 ± 0.03 L h^{-1} m^{-2}, over four continuous runs. Moreover, the membrane makes degradation faster by concentrating the pollutant during filtration. Our technology is effective in the production of pure water without creating a toxic concentrate, it relies on simple process design, and it does not require high pressure or additional chemicals. In addition, it can potentially work continuously driven by renewable thermal energies or waste heat.

npj Clean Water (2020)3:34 ; https://doi.org/10.1038/s41545-020-00082-2

INTRODUCTION

The increasing worldwide contamination of water systems caused by industrial development, climate change, population growth and over-consumption is one of the crucial environmental problems humanity is facing. Thousands of organic compounds which are often present in water at low concentrations (typically ng L^{-1} or μg L^{-1})[1] have become of significant concern, as they have been recognized as a major risk for humans, wildlife, and environment[2–4]. These contaminants of emerging concern are essentially pharmaceuticals, personal care products, steroid hormones, surfactants, industrial chemicals and pesticides, and their abatement cannot be achieved by the conventional physicochemical and biological treatments[5–8].

In this context, alternative treatments have been proposed for polluted wastewater streams. Among them, membrane filtration and advanced oxidation are gaining increasing attention, as they are highly effective in removing organic pollutants from water systems. Pressure-driven membrane filtration methods, such as nanofiltration and reverse osmosis, are well-established[9–11], but fouling and creation of toxic concentrates remain major drawbacks[12,13]. On the other hand, advanced oxidation processes[14–16], which are based on the generation of reactive oxygen species, offer the advantage of ideally mineralizing recalcitrant organic pollutants instead of simply concentrating them in the retentate. However, these processes often require substantial energy and/or chemical input, and their efficiency is limited by the high dilution of the micropollutants and by the non-toxic natural organic matter, which is typically present at high concentrations in wastewater and acts as radical scavenging[17]. The synergistic integration of advanced oxidation and membrane filtration can bring obvious benefits, because one method complements the advantages and overcomes the challenges of the other. For instance, nanofiltration has been proposed in combination with Fenton[18], photo-Fenton[19,20], and photocatalysis[21,22] to concentrate pollutants, thus improving degradation kinetics, while organics in the concentrate stream are fully mineralized. However, integrated photocatalytic-membrane systems are still complex and expensive for an implementation on a real scale, since they need to be activated by exposure to light with proper wavelength[23]. Therefore, their application cannot be extended to the existing wastewater treatment plants, which require technologies with low investment costs, low-energy consumption, high water productivity, and easy operation[24].

Here we present a novel process for simultaneous membrane distillation (MD) and thermocatalytic destruction of a model organic pollutant in the concentrate stream. This novel process is based on the integration of two emerging technologies for water treatment, namely membrane distillation and advanced oxidation by a thermocatalytic perovskite. In MD, a vapor pressure gradient is established between the hot feed side and the cold permeate side, which are divided by a porous hydrophobic membrane. Consequently, part of the feed vaporizes through the hydrophobic membrane and condenses at the permeate side, while dissolved salts and pollutants are retained. MD operates at much lower hydrostatic pressure than nanofiltration and reverse osmosis, thus allowing for simpler and cheaper filtration modules. In addition, permeability and selectivity of MD membranes are negligibly affected by osmotic pressure and fouling[25,26]. Regarding the advanced oxidation process, certain types of perovskites have been shown to interact with water and dissolved molecular oxygen to form reactive oxygen radicals, which can degrade organic pollutants[27]. Thermocatalytic perovskites have no need for addition of chemicals or light sources and therefore they demonstrate advantages over the other advanced oxidation processes in terms of energy saving and simplicity of operation. For instance, strontium ferrate ($SrFeO_{3-\delta}$) could achieve 83% mineralization of the endocrine distruptor bisphenol A (BPA) in 24 h, and full decoloration of the organic dye acid orange 8 in

[1]Center for Membrane Technology, Department of Chemistry and Bioscience, Aalborg University, Fredrik Bajers Vej 7H, DK-9220 Aalborg East, Denmark. [2]Istituto per lo Studio dei Materiali Nanostrutturati, Consiglio Nazionale delle Ricerche, Via Ugo La Malfa 153, 90146 Palermo, Italy. [3]Dipartimento di Chimica, Universitá di Torino, Via P. Giuria 7, 10125 Torino, Italy. [4]NIS Interdepartmental Centre, Universitá di Torino, Via P. Giuria 7, 10125 Torino, Italy. ✉email: vb@bio.aau.dk

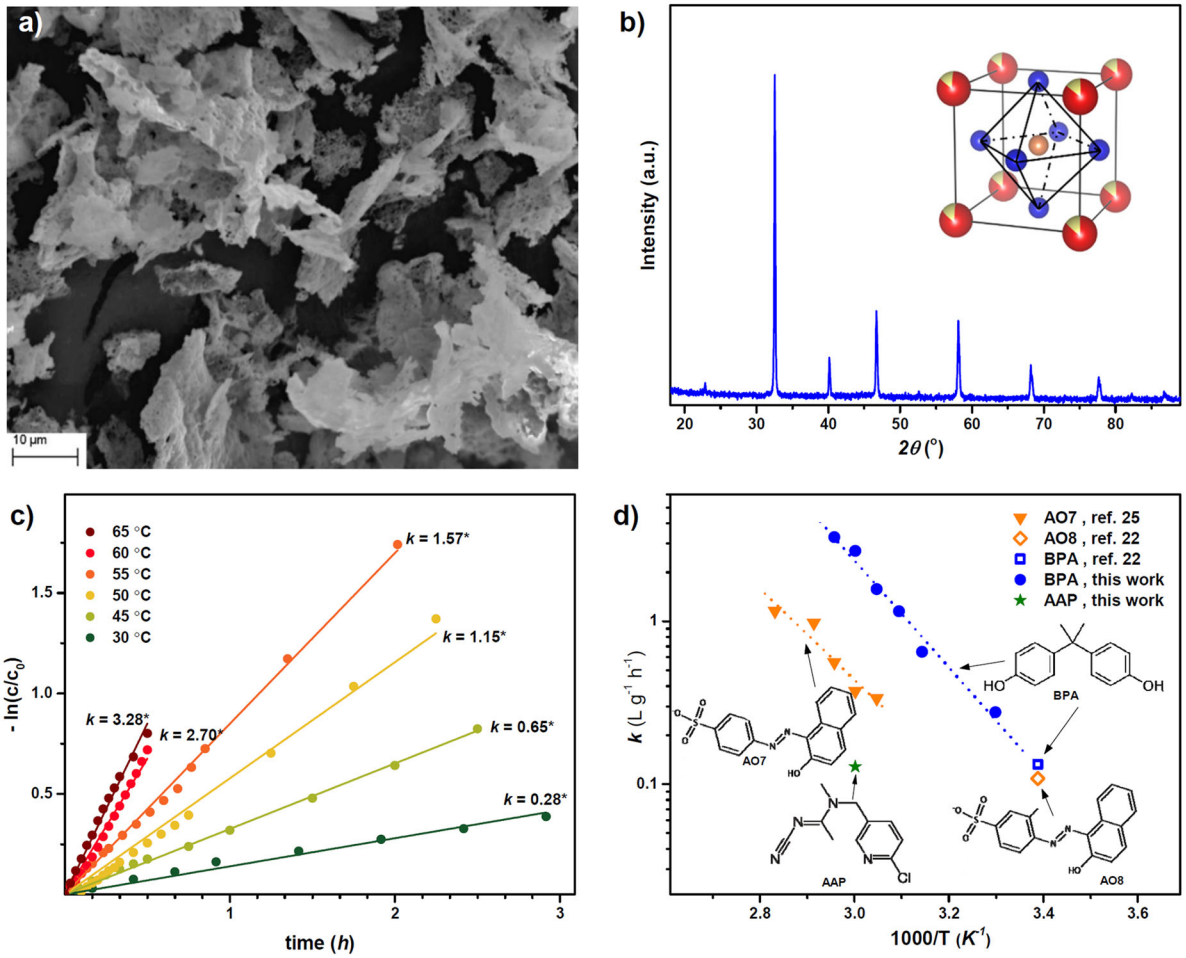

Fig. 1 Thermocatalytic abatement of micropollutants by cubic strontium ferrates. a SEM micrographs of $Sr_{0.85}Ce_{0.15}FeO_{3-\delta}$ (CSF) after calcination at 1000 °C and **b** the correspondent X-ray diffractogram. The image of the cubic perovskite structure as calculated by Rietveld refinement of the diffraction data is depicted in the right-up corner (the iron octahedral site of the $Sr_{0.85}Ce_{0.15}FeO_{3-\delta}$ perovskite is highlighted, whereas the orange, red, yellow, and blue spheres indicate iron, strontium, cerium, and oxygen atoms, respectively); **c** influence of temperature on the degradation of bisphenol A (initial concentration $c_0 = 10\ mg\ L^{-1}$) by $Sr_{0.85}Ce_{0.15}FeO_{3-\delta}$ ($0.50\ g\ L^{-1}$) and correspondent apparent rate constants, k ($L\ g^{-1}\ h^{-1}$); **d** temperature-dependence of kinetic constants for the abatement of model micropollutants by cubic strontium ferrates: bisphenol A (BPA), acid orange 7 (AO7), acid orange 8 (AO8), and acetamiprid (AAP).

60 min[28]. The redox-active cubic structure of strontium ferrate can be stabilized by cerium-doping[29,30]. Thus, Tummino et al.[31] used $Sr_{0.85}Ce_{0.15}FeO_{3-\delta}$ (cerium-doped strontium ferrate, CSF) to fully mineralize the organic dye acid orange 7 at temperatures ranging from 55 to 80 °C in few hours, in the dark and without adding chemicals. In our work, CSF was combined with MD to simultaneously degrade BPA while recovering distilled water. BPA was chosen as a model compound, because it is a common micropollutant[32] with a well-documented endocrine-disrupting activity and toxicity[33]. In this work, we heated the water contaminated by BPA at mild temperatures (30–65 °C) to facilitate the degradation process by CSF and to drive steam through a hollow fiber polypropylene MD membrane, simultaneously. The membrane retained both pollutant and thermocatalyst while producing distilled water, thus improving the degradation kinetics and allowing the thermocatalyst to be reused for several degradation cycles.

In a general perspective, thermocatalytic MD represents a new method for obtaining high purity distillate from contaminated waters, while also reducing the toxicity posed by organic compounds in the concentrate stream. The process design is simple, because it does not require high pressure, external light sources, or additional chemicals, and to the extent that MD is commercially scalable as a water treatment technology, so should be thermocatalytic MD. The process can be easily operated, because heat drives both thermocatalytic degradation of the pollutants and the permeation of distilled water through the membrane. Although part of this thermal energy is lost along the membrane module, energy costs can be compensated by using alternative heating sources, such as solar, geothermal, or low-grade waste heat from process streams[34,35]. Moreover, thermocatalytic MD can be applied to hot streams of polluted water generated by the chemical and the petrochemical industry.

RESULTS

Thermocatalytic abatement of micropollutants

Thermocatalytic CSF was prepared by solution-combustion synthesis[29,31], because this method can yield perovskites with well-defined properties[36]. SEM analysis (Fig. 1a) shows that our thermocatalytic powder consists of flakes with lateral dimension ranging from 1 to 30 µm and thickness smaller than 0.2 µm, as reported previously for CSF synthetized with the same method[31]. Such type of particles can easily be retained by membranes for microfiltration and MD. In addition, light scattering analysis revealed that when dispersed in water these particles tend to

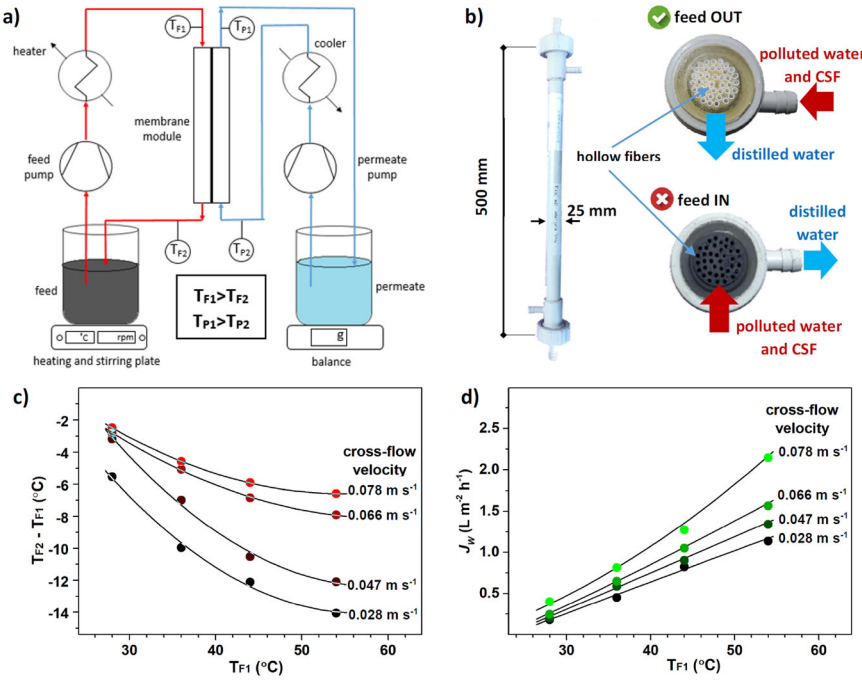

Fig. 2 Production of clean water by membrane distillation. a Scheme of the membrane distillation (MD) apparatus used in our experiments. The membrane module **b** consists of 40 porous polypropylene hollow fibers (length: 500 mm, inner diameter: 1.8 mm, wall thickness: 120 µm, and pore size: 0.2 µm). **c** The section of two membrane modules after being used with the correct flow configuration (feed OUT) and after being clogged by CSF particles (feed IN). T_{P2} was kept constant at ~17 °C in all the experiments, while T_{F1} and the cross-flow velocity were varied. The cross-flow velocity has an impact on **c** the drop of the feed temperature along the module and therefore **d** on the rate of water permeation through the membrane. In the plots, lines represent modeled values whereas bullets are measured values.

form aggregates with sizes of several microns, which makes it easy to recover them during filtration (Supplementary Fig. 1). The CSF particles also show a large density of macropores, which were presumably formed by gas-release during the combustion in the synthesis process.[36] The specific surface area of the material is 25 $m^2\,g^{-1}$, as measured by nitrogen adsorption (Supplementary Fig. 2). EDS analysis indicates a Ce:Fe atomic ratio of 0.15:1, confirming the cerium loading expected from the stoichiometry of the precursors' solution used for the synthesis. Figure 1b reports the X-ray diffractogram of CSF, which indicates that all the cerium ions have been incorporated in one crystal phase with cubic structure (*Pm-3m*). Particle size and shape, composition, porosity and crystal structure well match the $Sr_{0.85}Ce_{0.15}FeO_{3-\delta}$ perovskite previously reported by using the same preparation methodology[29,31], demonstrating the high reproducibility of the synthesis method.

The ability of the CSF to degrade BPA was investigated in temperatures ranging from 30 to 65 °C and thermocatalyst concentrations (C_{CSF}) between 0.15 and 1.0 g L^{-1}. Figure 1c shows the data obtained for the tests with $C_{CSF} = 0.50$ g L^{-1}. It was observed that CSF is highly active in the degradation of the BPA. Literature suggests that CSF can generate oxygen reactive species[28,31], but more investigation is required to determine the degradation mechanism. The BPA degradation process follows an apparent first-order kinetic with respect to catalyst and BPA concentrations. The rate constants are plotted as a function of the temperature in Fig. 1d. The observed degradation rate constant can be expressed according to following equation:

$$k = a \cdot C_{SCF} \cdot \exp\left(-\frac{E_a}{R \cdot T}\right) \quad (1)$$

In our BPA degradation experiments the frequency constant (a) and the apparent activation energy (E_a) resulted to be $(1.6 \pm 0.1) \times 10^{10}$ L g^{-1} h^{-1} and 63 ± 4 kJ mol^{-1}, respectively.

We determined BPA abatement rate constants with a trend consistent with the results that Leiw et al.[28] obtained with cubic strontium ferrate ($SrFeO_{3-\delta}$): i.e. $k = 0.13$ L g^{-1} h^{-1}, at room temperature. Moreover, cubic strontium ferrates have also proven their activity in the degradation of other model micropollutants, as shown in Fig. 1d. Leiw et al.[28] reported the ability of cubic $SrFeO_{3-\delta}$ to degrade the organic dye Acid Orange 8 at room temperature, after one day exposure (at room temperature $k =$ 0.11 L g^{-1} h^{-1}). Tummino et al.[31] performed a kinetic study of the degradation of Acid Orange 7 with CSF, determining an activation energy of 52 kJ mol^{-1}. Moreover, our CSF was able to degrade the pesticide Acetamiprid at a rate similar to the other pollutants ($k =$ 0.13 L g^{-1} h^{-1} at 60 °C).

Water purification by MD

In this work, we tested BPA degradation by CSF during filtration in a direct-contact MD apparatus, whose scheme is depicted in Fig. 2a. The hollow fiber membrane module used for our tests is shown in Fig. 2b. The module can function either by pumping the feed inside the hollow fibers and the permeate on the shell side or vice versa. However, when the feed solution flowed through the hollow fibers, the CSF powder clogged them after few hours of filtration. Therefore, all our tests were run with the feed solution flowing outside the hollow fibers, i.e. at the shell side. The rate of permeation of water through the membrane (J_W) was investigated at various feed temperatures and cross-flow velocities, while no pressure gradient was applied across the walls of the hollow fibers. On the contrary, a temperature gradient was established between the feed and the permeate side. However, this temperature gradient is not constant along the membrane module. Indeed, the feed temperature drops while flowing in the module due to two main factors: (i) the vaporization of water through the membrane pores and (ii) the convective heat transfer via the membrane walls. This drop in temperature ($T_{F2} - T_{F1}$) can

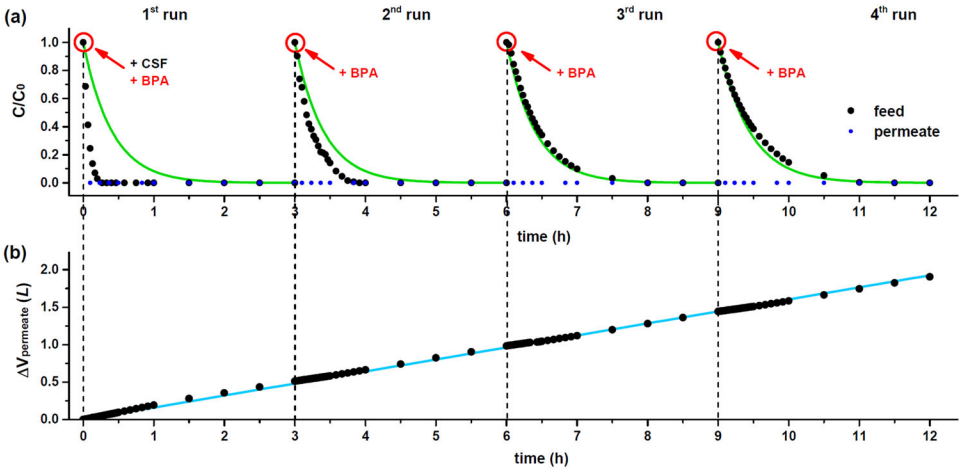

Fig. 3 Simultaneous degradation of BPA and production of distilled water by thermocatalytic membrane distillation with $Sr_{0.85}Ce_{0.15}FeO_{3-\delta}$ (CSF). a Concentration of BPA in the feed and in the permeate relatively to the starting BPA concentration in the feed tank, i.e. $C_0 = 10\ mg\ L^{-1}$, during four consecutive runs of thermocatalytic distillation in our apparatus, green lines represents BPA concentration in the feed, as calculated by our catalytic membrane distillation model (Supplementary Information, p. 4); **b** distilled water produced by our apparatus during the four runs, the blue line indicates the volume of permeated water over the entire thermocatalytic distillation experiment, as calculated by Eq. (2).

be reduced by increasing the cross-flow velocity (Fig. 2c). For instance, by setting T_{F1} to 54.0 °C, the feed temperature after leaving the module (T_{F2}) is 40.0 and 48.4 °C for cross-flow velocities of 0.028 and 0.078 m s^{-1}, respectively. In general, high cross-flow velocities are beneficial to preserve a water vapor pressure gradient across the membrane by reducing temperature drop from inlet to outlet of the filtration module and by mitigating temperature polarization at the membrane surface[37–45]. This results in higher water permeation rates (Fig. 2d). We observed no significant differences of water permeation rates in the experiments performed in the presence or in the absence of CSF powder (Supplementary Fig. 3) and our water fluxes are comparable with those reported in literature with the same membrane modules[46], suggesting that the CSF powder remains suspended in the solution feed and no cake layer is formed on the membrane surface. Based on these data, we developed an empirical model, which describes the temperature dependency of permeate flux. For instance, at a cross velocity of 0.047 m s^{-1}, permeate flux can be described by Eq. (2) (correlation coefficient with experimental data $R^2 = 0.991$), where ΔT represents the temperature difference [K] between the water in the feed beaker and the water in the permeate beaker.

$$J_W = 0.0022 \cdot \Delta T^{1.687} \quad (2)$$

Hence, by combining Eq. (1) and permeation data, we constructed a simple model for designing thermocatalytic MD for BPA abatement in our apparatus. A detailed description of this model is given in the Supplementary Information.

BPA abatement by thermocatalytic MD

The use of CSF in the MD apparatus (Fig. 2a) for simultaneous BPA abatement and clean water production is here evaluated. The experimental procedure was the following: at first, 1.80 L of a feed solution containing BPA ($C_0 = 10\ mg\ L^{-1}$) in deionized water was heated and kept at 65 °C. In the permeate reservoir, 0.50 L of distilled water was cooled by a water bath at 17 °C. The membrane cross-flow velocity was set to 20 L h^{-1} on both feed and permeate sides. Once the target temperatures were reached in both feed and permeate reservoirs, 1.8 g of CSF powder was added at once to the feed. The amount of water permeated through the membrane during the experiment was measured by a scale under the permeate beaker. Samples were taken at regular time intervals and analyzed by HPLC to determine BPA concentrations in the feed and in the permeate. After running the thermocatalytic distillation for 3 h, a new cycle was started. Thus, the required amounts of distilled water and BPA was added to the feed in order to reestablish the initial feed volume (1.80 L) and the BPA concentration (10 mg L^{-1}).

Figure 3a shows the relative concentration of BPA (C/C_0) plotted as a function of time over four consecutive runs. The membrane showed good retention of BPA along all the experiments, since the concentration of BPA in the permeate was always below the detection limit (0.05 mg L^{-1} in our analytical method, implying a BPA retention >99.5% at the start of each run). Such resistance to wetting for this membrane module is consistent with our previous results[46,47]. CSF was added at the feed side only at the beginning of the first run. Experimental data in the third and fourth runs fits well to our thermocatalytic MD model, while the observed degradation rates in the first and second runs were faster than expected. This discrepancy is probably caused by the fact that, at the beginning, all the CSF powder is dispersed in the water inside the feed beaker, which has a temperature of 65 °C. Then, part of the CSF powder migrates together with the feed solution inside the membrane module, where the average temperature of the water at the shell side is about 45 °C, as we have discussed already, thus reducing the degradation rate of BPA. Our model takes into account this temperature drop in the membrane modules, but our apparatus reaches steady-state only after a few hours of operation, that is, from the third run in Fig. 3a. We performed a control experiment in the absence of CSF, observing an increase in BPA concentration at the feed side during filtration (Supplementary Fig. 4). Furthermore, as already mentioned, the presence of the thermocatalyst does not affect the production rate of distilled water through our membrane and in Fig. 3b we can observe that the permeate production (J_W) was constant during the whole filtration experiment. Indeed, the linear fitting of all the experimental data points allowed to calculate $J_W = 1.60 \pm 0.03$ L h^{-1} m^{-2} ($R^2 = 0.9997$). Moreover, our model can well predict the water permeation rate under these experimental conditions: $J_W = 1.62$ L h^{-1} m^{-2}, according to Eq. (2).

The model was also used to investigate the impact of CSF loading and membrane area on the BPA abatement by thermocatalytic MD. Figure 4 reports our simulations. With no thermocatalytic perovskite (CSF) the BPA is concentrated during filtration. However, Fig. 4b shows that such increase in BPA concentration is

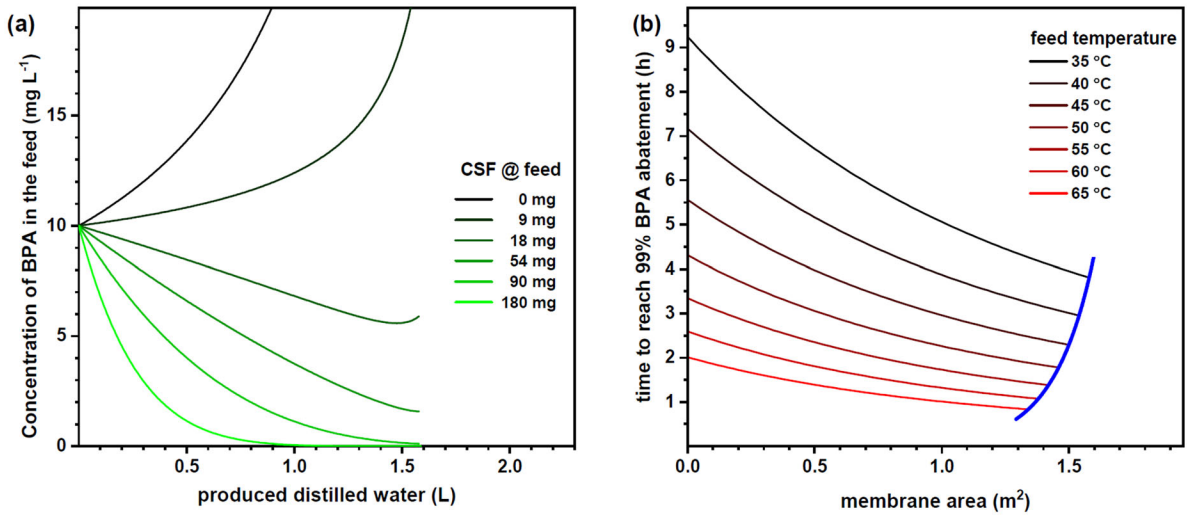

Fig. 4 Simulation of BPA abatement by the thermocatalytic membrane distillation. a BPA concentration in the feed as a function of the produced water at different CSF loadings (feed initial volume: 1.80 L, cross-flow velocity: 0.047 m s^{-1}, and temperatures in the feed and permeate beakers: 65 and 15 °C, respectively); **b** time needed to reach 99% degradation of BPA (initial C_{BPA}: 10 mg L^{-1}, CSF loading: 1.80 g) vs. membrane area at different feed temperatures. The blue line indicates the membrane area above which the permeate flow is so high that 99% BPA abatement cannot be reached before draining all the water in the feed beaker.

avoided by adding 54 mg of CSF in the feed stream. Furthermore, 1.80 g of CSF allows achieving >99% pollutant degradation while producing 1 L of water. Figure 4b shows the time needed to reach 99% abatement of BPA in our apparatus at different feed temperatures in the range from 30 to 65 °C, supposing that the area of the distillation membrane could be varied progressively from 0 to about 1.5 m^2. The blue line indicates the area at which, based on our simulation, the flow of distilled water through the membrane is faster than the rate of degradation, meaning that there is not enough time to reach 99% degradation before the feed beaker becomes empty. The graph makes evident the positive influence of larger membrane area on reducing the abatement time, explained by the membrane concentrating the pollutant during its abatement. The positive effect of the membrane is more pronounced at lower temperatures, where the degradation rates are slower. For instance, at 35 °C 99% BPA abatement is achieved in 9.2 h without membrane, while this time is reduced to 5 h by applying a membrane with area of 1 m^2.

DISCUSSION

For the first time a thermocatalytic perovskite with formula $Sr_{0.85}Ce_{0.15}FeO_{3-\delta}$ (CSF) was integrated in a MD unit. The new process was investigated in the degradation of BPA as a model water contaminant. A temperature-dependent catalytic behavior was confirmed for the CSF toward BPA degradation and its reusability was established up to four thermocatalytic distillation runs. In comparison with traditional pressure-driven filtration processes as nanofiltration and reverse osmosis, thermocatalytic MD offers the advantages of full BPA rejection, much lower operating pressure and, above all, the production of pure water without creating a toxic concentrate. Moreover, we proved that the combination of MD with CSF has advantages over the CSF batch catalysis. Indeed, the combined process is faster in the degradation of pollutants and it allows the recovery of the catalyst without additional steps, leading to higher clean water throughputs. Compared to photocatalytic membrane systems, the new process has no need of light irradiation and can be simply operated, as both MD and CSF are activated by heat. This is the first attempt to integrate MD with a thermocatalyst and the new technology still presents some challenges. Firstly, despite the kinetic constants for BPA degradation for CSF under dark conditions have the same magnitude of those observed for the traditional TiO_2 photocatalysts under UV light[48–51], our perovskite contains cerium, which makes it intrinsically more expensive than TiO_2. Moreover, the perovskite was synthetized by the solution-combustion method, which is a well-established and reproducible lab-scale procedure. Nevertheless, industrial production of the perovskite would require scale-up optimization. Deganello et al. analyzed this issue and proposed some solutions in a recent review[36]. Second, thermocatalytic materials have been shown to be effective in the abatement of model water pollutants or specific water systems and for operation time not longer than a few days[52], but the stability of their performances when treating wastewater effluents for several months (as in real applications) still needs to be explored. Third, MD apparatuses demand a substantial amount of thermal energy in order to heat and keep the temperature of the water at the feed side of the membrane, making MD economically viable only in the presence of cheap sources of heat. Despite these challenges, our experimental data allow for envisaging future optimization of the new process, e.g. by coupling MD modules with continuous stirred thank (Supplementary Information, p. 6) or with a fixed-bed thermocatalytic reactor in view of future applications with real water systems, for which the present literature[26,28,52] supports the feasibility of our technology. Therefore, this work may open the way to a new technology of the treatment of wastewater streams, stimulating the development of thermocatalysts with high-stability and activity for the degradation of a broad spectrum of micropollutants in complex water matrixes, MD units with high water productivity and new design solutions for the integrated system.

METHODS

CSF synthesis

1.80 g strontium (II) nitrate anhydrous (AVOCADO Research Chemicals Ltd, purity 99%), 4.04 g iron (III) nitrate nonahydrate (Sigma Aldrich, purity ≥98%) and 0.65 g cerium (III) nitrate hexahydrate (Sigma Aldrich, purity 99%) were dissolved in 200 mL of distillated water. Then, 7.68 g citric acid (Carl Roth, purity ≥99.5%) was added in order to reach a citric acid-to-metal cations ratio of 2, whereas the reducers-to-oxidizers ratio (Φ) was regulated at 1.5 through the addition of 9.25 g of ammonium nitrate (Sigma Aldrich, purity ≥99.5%) oxidant, according to the valence concepts based on propellant chemistry[36]. The pH of the solution was adjusted to 6.0 using ammonium hydroxide (Sigma Aldrich, 25 wt%), in order to favor citrate

anions–metal cations complex formation, and the glass beaker was placed on the hot plate and kept at 80 °C for the evaporation of the water under continuous magnetic stirring. When a sticky gel was obtained, the hot plate was set at the maximum temperature (310 °C) in order to start the gel self-ignition. After the combustion, the as-burned powder was calcined at 1000 °C for 5 h with a heating rate of 5 °C min^{-1}. After calcination, about 2 g of $Sr_{0.85}Ce_{0.15}FeO_{3-\delta}$ powder was obtained.

CSF characterization

X-ray diffraction (XRD) measurements were performed on a PANanalytical Empyrean diffractometer, operating at 45 kV and 40 mA, with Cu Kα radiation ($\lambda = 1.5418$ Å). $Sr_{0.85}Ce_{0.15}FeO_{3-\delta}$ was indexed in the Inorganic Crystal Structure Database (ICSD) under code #249012. CSF morphology was investigated by SEM analysis using a ZEISS EVO 50 XVP microscope with LaB_6 source. The samples were mounted on metallic stubs with double-sided conductive tape and ion coated with gold layer by a sputter coater (Baltec SCD 050) for 80 s under vacuum at a current intensity of 60 mA to avoid any charging effect. The chemical composition of samples was analyzed by energy-dispersive spectroscopy (EDS) using Oxford EDS INCA (Oxford Instruments). CSF specific surface area and porosity were determined by nitrogen adsorption/desorption isotherms at N_2 boiling point using an ASAP2020 gas-volumetric apparatus (Micromeritics). BET and BJH models were applied to calculate the specific surface area and pore size distribution, respectively. Prior to analyses, the samples were outgassed in vacuum (residual pressure ~ 10^{-2} mbar) at 300 °C. Particle size distribution was determined by laser diffraction using a particle size analyzer LS 13 320 single-wavelength (Beckman Coulter), with an analysis range from 0.37 to 2000 µm.

MD setup

The laboratory set-up was equipped with a Microdyn MD-020-2N-CP hollow fiber membrane module (nominal filtering area = 0.1 m^2) The set-up consisted of 1 L glass bottle of feed placed on heating plate with stirrer and 1 L bottle of permeate placed on balance. Feed and permeate were pumped through a peristaltic pump Masterflex L/S Easy-Load® (model 77200-62) from the feed bottle through heater followed by the membrane module and back into the feed tank. The flow rate of pumping was 20 L h^{-1}. Distilled permeate water was pumped from permeate bottle though a cooler and recirculated in the shell side ($d = 2.1$ cm) of the membrane module in a countercurrent mode, at a flow rate of 20 L h^{-1}. Both feed and permeate were recirculated back to their reservoirs, after passing through the contactor. The temperature was measured at the membrane inlet and outlet at the feed (T_F) and permeate (T_P) sides, where $T_{F1} > T_{F2}$ and $T_{P1} > T_{P2}$.

Degradation experiments

In batch tests performed to develop mathematical model, 200 mL of BPA solution (10 mg L^{-1} in deionized water) was poured in a 500 mL three neck round bottom flask immersed in an oil bath. The solution was heated under reflux to given temperature. After reaching set temperatures of 30, 45, 50, 55, 60. and 65 °C in each experiment, the perovskite was added to reach concentration of 0.5 g L^{-1} and the pH was adjusted to 7.0. Solution was continuously stirred and samples were taken on regular time intervals. To determine kinetic constant rates for different catalyst concentration the same experiment was performed in temperature 65 °C and the proper amount of perovskite was added each time to reach concentration of 0.15, 0.35, 0.75, and 1 g L^{-1}, respectively. The rate constant, k, values were determined for each temperature from the slope of the curve obtained when $-\ln(C_t/C_0)$ was plotted with respect to time. Results obtained from both experiments were used to determine our model and are described in the Supplementary material.

To determine the effectiveness of perovskite in degradation of BPA in the catalytic MD process, the experiment described in the following was performed. 1800 mL of feed solution containing BPA of concentration of 10 mg L^{-1} was prepared. The permeate initial volume consisted of 300 mL of distilled water. The volume of dead water needed to start the process was 200 mL. The feed was heated to 65 °C and the proper amount of perovskite was added to obtain concentration of 1 g L^{-1}. The pH was adjusted to 7.0 and the solution was under continuous stirring. The samples of feed and permeate were taken on regular intervals. For the experiment studying effectiveness of catalyst reuse in thermocatalytic MD process, the same procedure was repeated as described above, but the amount of catalyst needed to reach concentration of 1 g L^{-1} was added only in the first cycle. After addition, the solution of feed was heated to 65 °C, BPA was added at the beginning of each cycle to reach concentration of 10 g L^{-1} and pH was adjusted to 7.0. The procedure was repeated four times. In each experiment, collected samples were filtered using RC 0.45 µm syringe filters. Then, the liquid phases were analyzed through HPLC with UV detection (Summit-Dionex, with a Luna 5u C18 100 Å column (250 × 4.60 mm), mobile phase flow of 1 mL min^{-1} (acetonitrile/water = 60/40), UV detector at 230 nm) in order to determine the concentration of the contaminant in the sample. A calibration curve was determined using several solutions of BPA in concentrations between 1 and 10 mg L^{-1}.

DATA AVAILABILITY

The datasets generated during the current study are available from the corresponding author on reasonable request.

Received: 27 March 2020; Accepted: 29 June 2020;
Published online: 17 July 2020

REFERENCES

1. Schwarzenbach, R. P. et al. The challenge of micropollutants in aquatic systems. *Science* **5790**, 1072–1077 (2006).
2. Werber, J. R., Osuji, C. O. & Elimelech, M. Materials for next-generation desalination and water purification membranes. *Nat. Rev. Mater.* **1**, 16018 (2016).
3. Kim, S. et al. Removal of contaminants of emerging concern by membranes in water and wastewater: a review. *Chem. Eng. J.* **335**, 896–914 (2017).
4. Alvarez, P. J. J., Chan, C. K., Elimelech, M., Halas, N. J. & Villagrán, D. Emerging opportunities for nanotechnology to enhance water security. *Nat. Nanotechnol.* **13**, 634–641 (2018).
5. Serna-Galvis, E. A. et al. Degradation of seventeen contaminants of emerging concern in municipal wastewater effluents by sonochemical advanced oxidation processes. *Water Res.* **154**, 349–360 (2019).
6. Nawaz, T. & Sengupta, S. Contaminants of emerging concern: occurrence, fate, and remediation. In *Advances in Water Purification Techniques* (ed Ahuja, S.) 67–114 (Elsevier, 2019).
7. Bell, C. H. et al. *Emerging Contaminants Handbook* (CRC Press, 2019).
8. Fagan, R., McCormack, D. E., Dionysiou, D. D. & Pillai, S. C. A review of solar and visible light active TiO_2 photocatalysis for treating bacteria, cyanotoxins and contaminants of emerging concern. *Mater. Sci. Semicond. Process.* **42**, 2–14 (2016).
9. Żyłła, R., Boruta, T., Gmurek, M., Milala, R. & Ledakowicz, S. Integration of advanced oxidation and membrane filtration for removal of micropollutants of emerging concern. *Process Saf. Environ. Prot.* **130**, 67–76 (2019).
10. García Doménech, N., Purcell-Milton, F. & Gun'ko, Y. K. Recent progress and future prospects in development of advanced materials for nanofiltration. *Mater. Today Commun.* **23**, 100888 (2020).
11. Abdel-Fatah, M. A. Nanofiltration systems and applications in wastewater treatment: review article. *Ain Shams Eng. J.* **9**, 3077 (2018).
12. Li, N. et al. Comparing the performance of various nanofiltration membranes in advanced oxidation-nanofiltration treatment of reverse osmosis concentrates. *Environ. Sci. Pollut. Res.* **26**, 17472–17481 (2019).
13. Junussova, L. R. & Chicherin, S. V. Wastewater treatment and application in the advanced nanofiltration system. *IOP Conf. Ser. Earth Environ. Sci.* **408**, 012024 (2020).
14. Mayyahi, A. Al. & Al-asadi, H. A. A. Advanced oxidation processes (AOPs) for wastewater treatment and reuse: a brief review. *AJAST* **2**, 18–30 (2018).
15. Wang, J. A. Advanced oxidation processes for wastewater treatment: formation of hydroxyl radical and application. *Crit. Rev. Environ. Sci. Technol.* **42**, 251–325 (2015).
16. Espíndola, J. C. et al. Performance of hybrid systems coupling advanced oxidation processes and ultrafiltration for oxytetracycline removal. *Catal. Today* **328**, 274–280 (2019).
17. Hodges, B. C., Cates, E. L. & Kim, J.-H. Challenges and prospects of advanced oxidation water treatment processes using catalytic nanomaterials. *Nat. Nanotechnol.* **13**, 642–650 (2018).
18. Żyłła, R. & Kos, L. Application of Fenton reaction and nanofiltration for the recovery of process water. *Fibres Text. East. Eur.* **27**, 101–106 (2019).
19. Gallego-Schmid, A. et al. Environmental assessment of solar photo-Fenton processes in combination with nanofiltration for the removal of micro-contaminants from real wastewaters. *Sci. Total Environ.* **650**, 2210–2220 (2019).
20. Zhao, J., Ouyang, F., Yang, Y. & Tang, W. Degradation of recalcitrant organics in nanofiltration concentrate from biologically pretreated landfill leachate by ultraviolet-Fenton method. *Sep. Purif. Technol.* **235**, 116076 (2020).

21. Lv, Y. et al. Photocatalytic nanofiltration membranes with self-cleaning property for wastewater treatment. *Adv. Funct. Mater.* **27**, 1700251 (2017).
22. Janssens, R. et al. Coupling of nanofiltration and UV, UV/TiO_2 and UV/H_2O_2 processes for the removal of anti-cancer drugs from real secondary wastewater effluent. *J. Environ. Chem. Eng.* **7**, 103351 (2019).
23. Iervolino, G., Zammit, I., Vaiano, V. & Rizzo, L. Limitations and prospects for wastewater treatment by UV and visible-light-active heterogeneous photocatalysis: a critical review. *Top. Curr. Chem.* **378**, 7 (2020).
24. Nan, M., Jin, B., Chow, C. W. K. & Saint, C. Recent developments in photocatalytic water treatment technology: a review. *Water Res.* **44**, 2997–3027 (2010).
25. Quist-Jensen, C. A. et al. Direct contact membrane distillation for the concentration of clarified orange juice. *J. Food Eng.* **187**, 37–43 (2016).
26. Tijing, L. D. et al. Fouling and its control in membrane distillation—a review. *J. Memb. Sci.* **475**, 215–244 (2015).
27. Wang, Y. et al. Role of oxygen vacancies and Mn sites in hierarchical Mn_2O_3/$LaMnO_{3-\delta}$ perovskite composites for aqueous organic pollutants decontamination. *Appl. Catal. B* **245**, 546–554 (2019).
28. Leiw, M. Y. et al. Dark ambient degradation of bisphenol A and Acid Orange 8 as organic pollutants by perovskite $SrFeO_{3-\delta}$ metal oxide. *J. Hazard. Mater.* **260**, 1–8 (2013).
29. Deganello, F., Liotta, L. F., Longo, A., Casaletto, M. P. & Scopelliti, M. Cerium effect on the phase structure, phase stability and redox properties of Ce-doped strontium ferrates. *J. Solid State Chem.* **179**, 3406–3419 (2006).
30. Deganello, F., Liotta, L. F., Leonardi, S. G. & Neri, G. Electrochemical properties of Ce-doped $SrFeO_3$ perovskites-modified electrodes towards hydrogen peroxide oxidation. *Electrochim. Acta* **190**, 939–947 (2016).
31. Tummino, M. L., Laurenti, E., Deganello, F., Bianco Prevot, A. & Magnacca, G. Revisiting the catalytic activity of a doped $SrFeO_3$ for water pollutants removal: effect of light and temperature. *Appl. Catal. B* **207**, 174–181 (2017).
32. Dudziak, M. et al. Elimination of bisphenol A from wastewater through membrane filtration processes. *J. Ecol. Eng.* **19**, 69–74 (2018).
33. Zhang, K. et al. Degradation of bisphenol-A using ultrasonic irradiation assisted by low-concentration hydrogen peroxide. *J. Environ. Sci.* **23**, 31–36 (2011).
34. Alkhudhiri, A., Darwish, N. & Hilal, N. Membrane distillation: a comprehensive review. *Desalination* **287**, 2–18 (2012).
35. Zhang, Y., Rottiers, T., Meesschaert, B., Pinoy, L. & Van der Bruggen, B. Wastewater treatment by renewable energy driven membrane processes. In *Current Trends and Future Developments on (Bio-)* (eds Basile, A., Cassano, A. & Figoli, A.) *Membranes*. 1–19 (Elsevier, 2019).
36. Deganello, F. & Tyagi, A. K. Solution combustion synthesis, energy and environment: best parameters for better materials. *Prog. Cryst. Growth Charact. Mater.* **64**, 23–61 (2018).
37. Abo, R., Kummer, N. & Merkel, B. J. Optimized photodegradation of bisphenol A in water using ZnO, TiO_2 and SnO_2 photocatalysts under UV radiation as a decontamination procedure. *Drink. Water Eng. Sci.* **9**, 27–35 (2016).
38. Chiang, K., Lim, T. M., Tsen, L. & Lee, C. C. Photocatalytic degradation and mineralization of bisphenol A by TiO_2 and platinized TiO_2. *Environ. Sci. Technol.* **261**, 225–237 (2004).
39. Mahlambi, M. M., Ngila, C. J. & Mamba, B. B. Recent developments in environmental photocatalytic degradation of organic pollutants: the case of titanium dioxide nanoparticles—a review. *J. Nanomater.* **2015**, 790173 (2015).
40. Dükkancı, M. Degradation of bisphenol-a using a sonophoto Fenton-like hybrid process over a $LaFeO_3$ perovskite catalyst and a comparison of its activity with that of a TiO_2 photocatalyst. *Turk. J. Chem.* **40**, 784–801 (2016).
41. Dong, H., Zeng, G., Tang, L. & Fan, C. An overview on limitations of TiO_2-based particles for photocatalytic degradation of organic pollutants and the corresponding countermeasures. *Water Res.* **79**, 128–146 (2015).
42. Reddy, P. V. L. et al. Photocatalytic degradation of bisphenol A in aqueous media: a review. *J. Environ. Manag.* **213**, 189–205 (2018).
43. Jia, Y. et al. Nitrogen doped $BiFeO_3$ with enhanced magnetic properties and photo-Fenton catalytic activity for degradation of bisphenol A under visible light. *Chem. Eng. J.* **337**, 709–721 (2018).
44. Dükkancı, M. Sono-photo-Fenton oxidation of bisphenol-A over a LaFeO3 perovskite catalyst. *Ultrason. Sonochem.* **40**, 110–116 (2018).
45. Deshmukh, A. et al. Membrane distillation at the water-energy nexus: limits, opportunities, and challenges. *Energy Environ. Sci.* **11**, 1177–1196 (2018).
46. Moran Ayala, L. I. et al. Water defluoridation: nanofiltration vs. membrane distillation. *Ind. Eng. Chem. Res.* **57**, 14740–14748 (2018).
47. Lazar, M. A., Varghese, S. & Nair, S. S. Photocatalytic water treatment by titanium dioxide: recent updates. *Catalysis* **4**, 572–601 (2012).
48. Garg, A. et al. Photocatalytic degradation of bisphenol-A using N, Co codoped TiO_2 catalyst under solar light. *Sci. Rep.* **9**, 765 (2019).
49. Kuo, C. Y., Wu, C. H. & Lin, H. Y. Photocatalytic degradation of bisphenol A in a visible light/TiO_2 system. *Desalination* **256**, 37–42 (2010).
50. Gao, B., Lim, T. M., Subagio, D. P. & Lim, T. T. Zr-doped TiO_2 for enhanced photocatalytic degradation of bisphenol A. *Appl. Catal. A Gen.* **375**, 107–115 (2010).
51. Jia, C., Qin, Q., Wang, Y. & Zhang, C. Photocatalytic degradation of bisphenol A in aqueous suspensions of titanium dioxide. *Adv. Mater. Res.* **433–440**, 172–177 (2012).
52. Chen, H., Jiangang, K. & Wang, L. Thermal catalysis under dark ambient conditions in environmental remediation: fundamental principles, development, and challenges. *Chin. J. Catal.* **40**, 1117–1134 (2019).

ACKNOWLEDGEMENTS

This paper is part of a project that has received funding from the European Union's Horizon 2020 research and innovation program under the Marie Skłodowska-Curie grant agreement No. 765860.

AUTHOR CONTRIBUTIONS

V.B. conceived the concept, C.A.Q.-J. designed and built the MD setup and help designing experiments; K.J., F.E.B.C., and F.H. carried out materials synthesis and permeation tests. K.J., F.H., M.K.J., and V.B. analyzed data. F.E.B.C., F.D., and G.M. performed material characterization. M.K.J. and K.J. developed a model for the catalytic membrane distillation system; K.J. wrote the paper with editorial contributions from V.B., M.K.J., F.D., F.E.B.C., C.A.Q.-J., and G.M.

COMPETING INTERESTS

The authors declare no competing interests.

ADDITIONAL INFORMATION

Supplementary information is available for this paper at https://doi.org/10.1038/s41545-020-00082-2.

Correspondence and requests for materials should be addressed to V.B.

Reprints and permission information is available at http://www.nature.com/reprints

Publisher's note Springer Nature remains neutral with regard to jurisdictional claims in published maps and institutional affiliations.

Paper II

membranes

MDPI

Article

Combined Nanofiltration and Thermocatalysis for the Simultaneous Degradation of Micropollutants, Fouling Mitigation and Water Purification

Katarzyna Janowska [1], Xianzheng Ma [1], Vittorio Boffa [1,*], Mads Koustrup Jørgensen [1] and Victor M. Candelario [2]

[1] Center for Membrane Technology, Department of Chemistry and Bioscience, Aalborg University, Fredrik Bajers Vej 7H, 9220 Aalborg, Denmark; kaj@bio.aau.dk (K.J.); xm@bio.aau.dk (X.M.); mkj@bio.aau.dk (M.K.J.)

[2] Department of Research and Development, LiqTech Ceramics A/S, Industriparken 22C, 2750 Ballerup, Denmark; vcl@liqtech.com

* Correspondence: vb@bio.aau.dk; Tel.: +45-9940-3579

Abstract: Due to progressive limitation of access to clean drinkable water, it is nowadays a priority to find an effective method of water purification from those emerging organic contaminants, which might have potentially harmful and irreversible effects on living organisms and environment. This manuscript reports the development of a new strategy for water purification, which combines a novel and recently developed Al_2O_3-doped silica nanofiltration membrane with a thermocatalytic perovskite, namely cerium-doped strontium ferrate (CSF). The thermocatalytic activity of CSF offers the opportunity to degrade organic pollutants with no light and without input of chemical oxidants, providing simplicity of operation. Moreover, our studies on real samples of secondary effluent from wastewater treatment showed that the thermocatalyst has the ability to degrade also part of the non-toxic organic matter, which allows for reducing the chemical oxygen demand of the retentate and mitigating membrane fouling during filtration. Therefore, the new technology is effective in the production of clean feed and permeate and has a potential to be used in degradation of micropollutants in water treatment.

Keywords: nanofiltration; thermocatalysis; perovskite; micropollutants; water purification; wastewater

Citation: Janowska, K.; Ma, X.; Boffa, V.; Jørgensen, M.K.; Candelario, V.M. Combined Nanofiltration and Thermocatalysis for the Simultaneous Degradation of Micropollutants, Fouling Mitigation and Water Purification. *Membranes* **2021**, *11*, 639. http://doi.org/10.3390/membranes11080639

Academic Editor: Anthony Szymczyk

Received: 19 July 2021
Accepted: 16 August 2021
Published: 19 August 2021

1. Introduction

Sources of global, usable clean drinking water are dramatically decreasing and it is a lifeline to save our planet from a water crisis. Municipal, industrial and agricultural wastewaters are the main sources of micropollutants causing the contamination of natural and drinking water. These compounds such as personal care products, pesticides, pharmaceuticals, hormones, industrial chemicals and environmental estrogens, even at low concentrations (ng L^{-1} or µg L^{-1}), have damaging and irreversible effects on living organisms and the environment [1,2]. Therefore, it is a priority to develop an efficient technology to remove these contaminants from wastewater, considering that, in conventional wastewater treatment plants (WWTPs), physical methods are unproductive for their abatement [3], and biological processes can provide only a limited degradation of such pollutants [4,5]. Therefore, a number of advanced wastewater treatment technologies such as activated carbon adsorption, advanced oxidation processes and membrane technologies have been used for water purification [6]. Above all, membrane-based technologies are recently gaining attention as they produce water of superior quality, they are less sensitive to feed quality fluctuations, and their footprint is much smaller compared to conventional water treatment processes [4]. Out of membrane technologies, especially nanofiltration (NF) has been found as a promising cost-effective alternative method for

removing and concentrating low-molecular-weight organic micropollutants [7,8]. The pore sizes of NF membranes are typically between 1 and 2 nm, so they can molecularly sieve hydrated multivalent ions and organic micropollutants [9,10]. NF is distinguished by low operating pressure and high permeability, which benefits in the form of relatively low investment, operation and maintenance costs [11]. Nevertheless, there are some limitations of this process such as the non-complete rejection of water pollutants, membrane fouling, and the production of a toxic concentrate (retentate), which needs to be treated before disposal [2,6,8,12,13].

This manuscript reports the development of a novel strategy for water purification that involves the integration of membrane filtration and advanced oxidation. For filtration experiments, we used a ceramic membrane consisting of alumina tubular support coated with an Al_2O_3-doped NF silica layer, which has been previously reported [14], showing good retention of organic pollutants. Al_2O_3 doping was used to increase the chemical stability of the silica thin layer [14,15]. Moreover, the tubular configuration and the mechanical resistance of this membrane are suitable to perform the NF experiment in the presence of thermocatalytic particles, which might clog or scratch commercial polymeric membrane modules. Advanced oxidation processes (AOPs) utilize highly reactive oxygen species (ROS) such as OH• and O_2•-, which mineralize most of the pollutants into less or non-toxic products (e.g., H_2O and CO_2) in aqueous systems [3,16,17]. Among AOPs, thermal catalysis offers the opportunity to degrade organic pollutants with no light and without input of chemical oxidants. Therefore, in our experiments, the concentration of micropollutants and organic matter in the membrane retentates were reduced by treatment with a perovskite thermocatalyst, namely, cerium-doped strontium ferrate (CSF), either during or after filtration. Bisphenol A (BPA) was chosen as a model pollutant to spark water samples, because it is a common water contaminant with a well-documented endocrine-disrupting activity and toxicity [18]. Moreover, common biological treatments are not effective for BPA degradation [19]. On the other hand, we reported full abatement of BPA in water by treatment with CSF perovskite in our previous study [20].

The purpose of this work was to integrate a ceramic membrane with perovskite in order to effectively retain and degrade BPA and improve the quality of feed and permeate. We also performed tests with real secondary effluent from treatment wastewater, which contain large amounts of non-toxic organic matter. Organic matter may have a negative influence on the thermocatalytic abatement of micropollutants and can cause clogging of membranes' pores at the detriment of membrane permeance [21]. It is responsible for membrane fouling and for the chemical oxygen demand of the retentate. Therefore, the influence of the thermocatalyst on reduction of non-toxic organic matter content and fouling is also discussed. Finally, we performed a two-step experiment to check the impact of thermocatalyst on BPA abatement and organic matter degradation for effluent concentrate in order to compare it with one-step filtration with thermocatalyst addition.

2. Materials and Methods

2.1. Cerium-Doped Strontium Ferrate Perovskite Synthesis

Initially, 1.8 g strontium nitrate (Carl Roth, purity $\geq$ 99%), 4.04 g iron (III) nitrate (Sigma-Aldrich, purity $\geq$ 98%) and 0.65 g cerium (III) nitrate (Sigma-Aldrich, purity 99%) were completely dissolved in 200 mL of distillated water, using a 1 L glass beaker as container. Then, 7.68 g citric acid (Carl Roth, purity $\geq$ 99.5%) were added in order to reach a citric acid-to-metal cations ratio of 2, whereas the reducers-to-oxidizers ratio (Φ) was regulated at its stoichiometric value through the addition of 9.25 g of ammonium nitrate (Sigma-Aldrich, purity $\geq$ 99.5%), according to the valence concepts based on propellant chemistry [22]. The pH of the solution was adjusted to 6.0 using ammonium hydroxide (Sigma-Aldrich, 25 wt %), in order to favor citrate anions-metal cations complex formation, and the glass beaker was placed on a hot plate and kept under 80 °C for the evaporation of the water under continuous magnetic stirring. When a sticky gel was obtained, the hot plate was set to the maximum temperature (310 °C) in order to start the gel self-ignition. After

the combustion, the as-burned powder was calcined in 1000 °C for 5 h with a heating rate of 5 °C min^{-1}. After calcination, about 2 g of $Sr_{0.85}Ce_{0.15}FeO_{3-\delta}$ powder were obtained.

2.2. Membrane Fabrication

The membrane preparation method is described in detail by Ma et al. [14]. Note that 5% mol Al_2O_3-doped silica NF membrane used for tests was fabricated via the sol-gel method using a cationic surfactant, namely, N,N,N-Trimethylhexadecan-1-aminium bromide (CTAB) as pore-forming agent. The molar ratio of surfactant/oxide was kept at 0.5, because, based on the previous study, the membrane prepared under such conditions exhibited the best selectivity towards organic pollutants and salts. A two-step approach was applied for the sol synthesis. The first step of synthesis was the hydrolysis of TEOS, which was achieved by letting to react a mixture of TEOS (98%, Sigma-Aldrich, St. Louis, MO, USA), ethanol (99.9%, VWR Chemicals, Radnor, PA, USA), deionized water, and nitric acid (69%, Sigma-Aldrich, St. Louis, MO, USA), with a molar ratio of 1:4:2.5:0.04, at 60 °C for 3 h. Then, in the second step of the synthesis, CTAB (99%, Sigma-Aldrich, St. Louis, MO, USA) was added to the pre-hydrolyzed TEOS solution to achieve the desired CTAB: (SiO_2 + Al_2O_3) molar ratio. After the complete dissolution of CTAB, aluminum isopropoxide (AIP) (98%, Sigma-Aldrich, St. Louis, MO, USA) was directly added to the mixture to obtain a 5 mol% Al_2O_3 concentration in the final consolidated membrane material. The mixture was continuously stirred at 60 °C until all the AIP was dissolved and a transparent yellowish solution was obtained). Sol was diluted by 1:20 volume ratio with ethanol and subsequently filtered with a 0.2 µm syringe filter (Minisart RC, 25 mm, Sigma-Aldrich, St. Louis, MO, USA) to remove dust particles and impurities before the coating. The membrane was coated on commercial y-alumina tubular support with y-alumina intermedia layer (250 × 10 × 7 mm (L × OD × ID), Pervatech B.V., Rijssen, The Netherlands). The membrane was fabricated by dip-coating of the alumina-doped silica sols onto the supporting substrates. Specifically, the inside of the supports was coated vertical by a lab-made device at a dipping/withdrawing rate of <2.5 cm/min. After drying at room temperature for 24 h, the membranes were calcined at 450 °C for 2 h at the heating and cooling rate of 2 °C min^{-1}.

2.3. SEM

The morphology of the membrane cross-section and surface was investigated by SEM analysis using an EVO 50 XVP microscope (Zeiss, Köln, Germany) with LaB6 source. The samples were mounted on metallic stubs with double-sided conductive tape and ion coated with a gold layer (thickness ~25 nm) by a sputter coater (Baltec SCD 050, Pfäffikon, Switzerland) for 60 s under vacuum at a current intensity of 60 mA to avoid any charging effect.

2.4. Effluent Sampling

Secondary effluent was sampled from the Wastewater Treatment Plant Aalborg West (AAW) 57.049422° N, 9.864735° E in Denmark in January 2021. Sampling permission was granted by Aalborg Forsyning, Kloak A/S. Samples were transported to the laboratory within 1 h after sampling and kept in the fridge until experiments. Samples were used for NF permeance tests without and with addition of thermocatalyst and for experiments with concentrate.

2.5. Nanofiltration Apparatus

The experimental cross-flow filtration set-up is shown in Figure 1, and it follows the system described by Farsi et al. [23]. The feed was pumped to the NF membrane by a feed pump giving pressure 6 bar. Monotubular membrane (250 × 10 × 7 mm (L × OD × ID), Pervatech B.V., The Netherlands) was sealed completely in a stainless steel membrane module. The effective membrane surface was 55 cm^2. The permeate mass flow was measured by a balance (Mettler Toledo, Mono Bloc series, Greifensee, Switzerland) connected

to a computer to continuously log the weight of the permeate. The feed pressure was measured before and after the membrane by two pressure transmitters (Danfoss, MBS 4010, Nordborg, Denmark) and an electronic heat sensor (Kamstrup A/S, Skanderborg Denmark) measured feed temperature before membrane module. A rotary lobe pump (Philipp Hilge GmbH & Co, Novalobe, Germany) generated the cross-flow rate measured by a microprocessor-based flow rate transmitter (Siemens, MAG 50000, Munich, Germany). It was adjusted to 1.6 ± 1 m s^{-1} for all the experiments. The retentate stream was controlled by a manual valve. The system was operated for 3 h to ensure that the system was operated at steady-state condition. During filtration, samples were collected from each stream (feed, permeate) at various times to observe system changes during time. Filtration experiments were done at temperature 50 °C. A typical test started by filling up the feed tank with 1.8 L of solution and setting the system at the specified operational conditions.

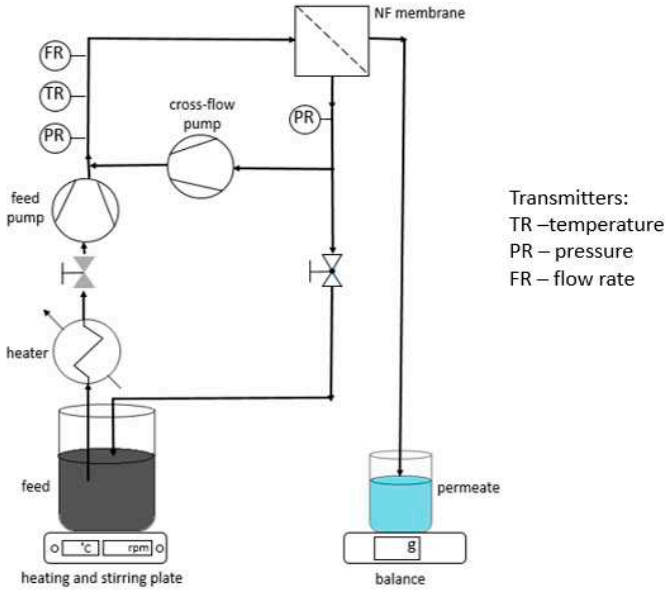

Figure 1. Scheme of the nanofiltration setup used in this study.

2.6. COD Analysis

COD (chemical oxygen demand) analysis was performed using COD kits (Hach®) 5–60 mg/L and 15–150 mL/L and Hach Lange DR3900 apparatus. Then, 2 mL of samples were added to each vial from the proper kit and placed in a heating block for 2 h at 148 °C. After cooling down to 20 °C, the vials were placed one after another in Hach Lange to measure COD in mg L^{-1}.

2.7. Determination of BPA Concentration in Water Samples

In each experiment, collected samples of feed were filtered using RC 0.45 µm syringe filters. Then, the liquid phases of feed and permeate were analyzed through HPLC with UV detection (Phenomenex, with a Kintex® 5 µm EVO C18 100 Å LC column (150 × 4.60 mm), mobile phase flow of 1 mL min^{-1} (acetonitrile/water = 60/40 v/v%), UV detector at 230 nm) in order to determine the concentration of the contaminant in the sample. A calibration curve was determined using several solutions of BPA in concentrations between 1 and 10 mg L^{-1}.

3. Results

3.1. SEM of Membrane

Figure 2 shows the SEM cross-section of the Al_2O_3-doped silica membrane used in this study. The micrograph shows a continuous film covering the multilayered alumina support. From the picture, the thickness of the top layer measured to be 0.5 µm. Based on

analysis at the low-temperature porosimeter [14], the Al_2O_3-doped silica material coated on the alumina support has main and maximum pore size of 1.3 nm and 2.5 nm, respectively, and therefore it is suitable to act as a NF membrane. Moreover, CSF particles have a flake-like structure with thickness of about 0.2 µm and lateral dimensions that are several micrometers large. Therefore, Al_2O_3-doped silica membrane can easily retain CSF particles at the feed side during filtration.

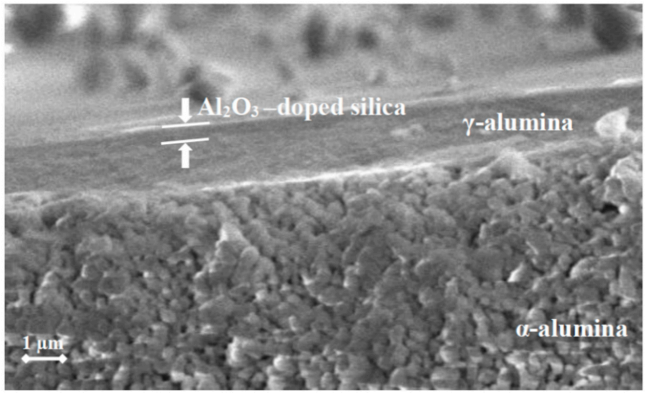

Figure 2. Cross-sectional SEM micrograph of the membrane used in this study. The Al_2O_3-doped silica NF layer is coated over a mesoporous γ-alumina interlayer and a macroporous α-alumina support.

3.2. BPA Rejection

The experiment studying the BPA rejection and impact of temperature on water permeance was performed using 1.8 L of deionized water with a starting BPA concentration of 10 mg L^{-1} as membrane feed. The cross flow was set up to 1.6 ± 0.1 m s^{-1} and the feed was pumped with a trans-membrane pressure of 6 bar. From Figure 3, it can be seen that no impact of temperature on BPA rejection has been observed. Pollutant rejection remains constant, reaching values near to 100% at all the tested temperatures: 30 °C (98.7%), 40 °C (99.5%), 50 °C (98.6%), 55 °C (98.8%), 60 °C (98.9%). However, the water permeance of the membrane increased with increase of temperature in the range 30–60 °C as follows: 30 °C (1.09 L (h m^2 bar)$^{-1}$), 40 °C (1.40 L (h m^2 bar)$^{-1}$), 50 °C (1.91 L (h m^2 bar)$^{-1}$), 55 °C (2.02 L(h m^2 bar)$^{-1}$), 60 °C (2.17 L (h m^2 bar)$^{-1}$). This twofold increase of water permeance from 30 to 60 °C is consistent with the data reported by Tsuru et al. [24] for other types of ceramic NF membranes.

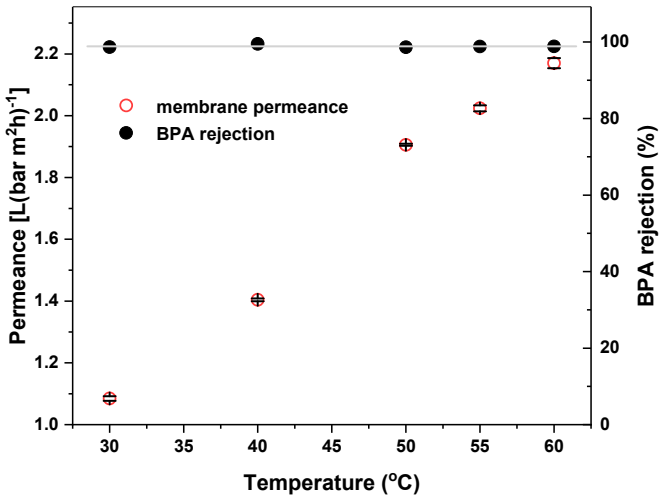

Figure 3. Impact of temperature on water permeance and BPA rejection for the Al_2O_3-doped silica NF membrane used in this study. Black bars indicate the error for the permeance values.

3.3. BPA Abatement during Filtration

The experiments to investigate the thermocatalytic abatement during filtration were performed at a temperature of 50 °C, because our previous studies showed that CSF can catalyze fast degradation of BPA at this temperature [20]. The feed volume was 1.8 L, a cross flow of 1.6 ± 0.1 m s^{-1} was applied and the transmembrane pressure was 6 bar. The feed was heated and after reaching a temperature of 50 °C the proper amount of BPA was added to reach a concentration of pollutant of 10 mg L^{-1}. After running the system for 2 h, the thermocatalyst was added in the retentate to reach a concentration of 1 g L^{-1} and the system was operated for another 3 h.

In Figure 4a, it can be seen that during the first 2 h the concentration of BPA in the feed was stable at about 10 mg L^{-1}, with a slight increase, which corresponds to the volumetric concentration factor (VCF), i.e., the ratio of the initial feed volume to the feed volume after a certain filtration time. Indeed, in our filtration experiment, VCF was only 1.069 after 2 h of filtration. Hence, the BPA concentrations in the feed during the first two hours indicate that this micropollutant is stable at the filtering temperature. On the contrary, after adding the CSF thermocatalyst, the concentration of BPA immediately decreases, reaching 4 g L^{-1} after 3 h of operation, despite a VCF = 1.241 for this filtration time.

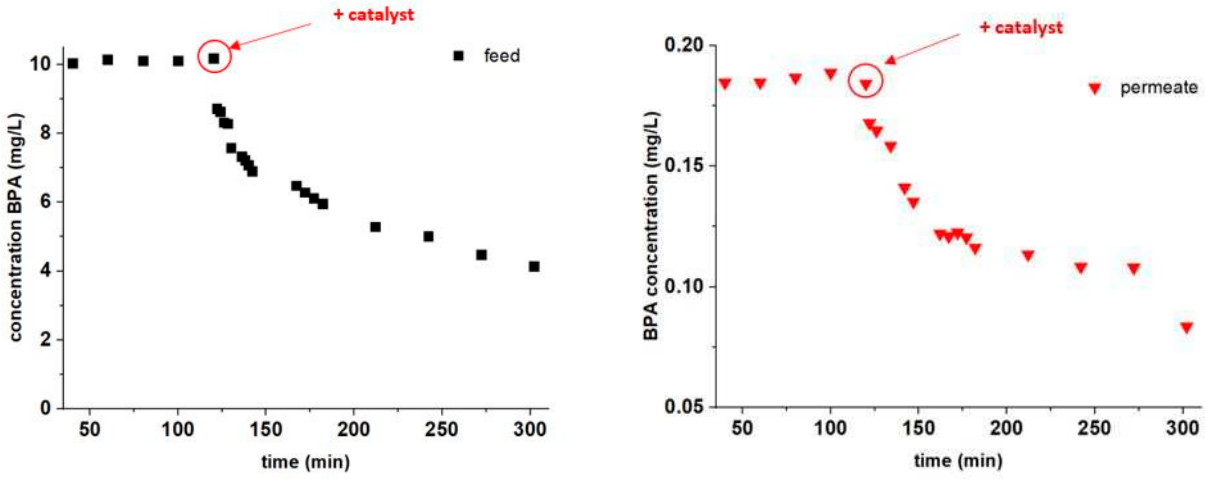

(**a**) (**b**)

Figure 4. Degradation experiment at 50 °C with addition of CSF: (**a**) BPA concentration in the membrane feed as a function of the filtration time; (**b**) BPA concentration in the permeate as a function of the filtration time. Red arrows and circles indicate the time when CSF was added to the membrane feed solution.

Figure 4b shows the development in concentration of BPA in the permeate over time. It can be seen that, during the first 2 h, the permeate concentration of BPA is stable, around 0.19 mg L^{-1}, with a slight increase, which corresponds to the increase in concentration at the retentate side. After adding the thermocatalyst to the feed, the concentration of BPA in the permeate significantly decreases, reaching about 0.1 mg L^{-1} after 3 h. This experiment proves that the addition of thermocatalyst to the NF system leads not only to the abatement of BPA at the feed side, but it also improves the quality of the permeate. Indeed, the membrane selectivity remains constant at (98.1 ± 0.2)% during this filtration experiment (when excluding the outlying value measured for the permeate at 300 min). Therefore, the abatement of BPA concentration at the feed side, upon adding the CSF powder, corresponds to a decrease in BPA concentration at the permeate side. Moreover, the addition of CSF powder did not undermine BPA rejection, suggesting that CSF particles had not damaged the Al-doped silica NF layer (e.g., by friction) during the experiment.

3.4. Fouling Mitigation

The experiments to investigate the influence of thermocatalyst on the reduction of non-toxic organic matter and fouling were conducted by filtering the secondary effluent collected from the Aalborg Wastewater Plant West (WWTP). The properties of effluent are listed in Table 1.

Table 1. Properties of effluent.

Parameter	Unit	Value
pH (22.0 °C)		7.48 ± 0.01
Conductivity (22.5 °C)	mS/cm	1.15 ± 0.01
COD	mg/L	33.4 ± 0.7

As can be seen in Figure 5, when the NF membrane is used to filter a real wastewater effluent, the flux of the permeate decreases along the filtration time. The 80% of permeate flux decline can be explained by the membrane being fouled by the organic matter present in the wastewater effluent (COD 33.4 mg L^{-1}). On the other hand, the flux decline of the permeate was only 20% when 1 g L^{-1} of CSF was added to the wastewater effluent during filtration. Moreover, the fouling was studied to determine which fouling type occurred during each experiment. A method based on a simple regression fitting [25] was used to determine the type of fouling mechanisms in experiments on the filtration with cross flow, as explained in detail in the Supplementary Materials. It was found that, for both the effluent with and without thermocatalyst, the main fouling type is intermediate pore blocking, for which the best (≈1) R^2 correlations were found. It can be seen in Figure 5 that modelled data correspond well with the experimental data for filtration of effluent with (J_{SS} = 2.704 L m^{-2} h^{-1}, K_i = 0.009) and without thermocatalyst (J_{SS} = 0.816 L m^{-2} h^{-1}, K_i = 0.004). The intermediate pore blocking appeared to give slower fouling formation for experiments with thermocatalyst, which is explained by the lower content of organic matter to fouling the membrane as a result of organic matter degradation by the thermocatalyst. After about 100 min of filtration, the models deviate from intermediate pore blocking models, which may be a result of cake formation [25], which in this case can correspond to deposition of CSF particles on the membrane surface.

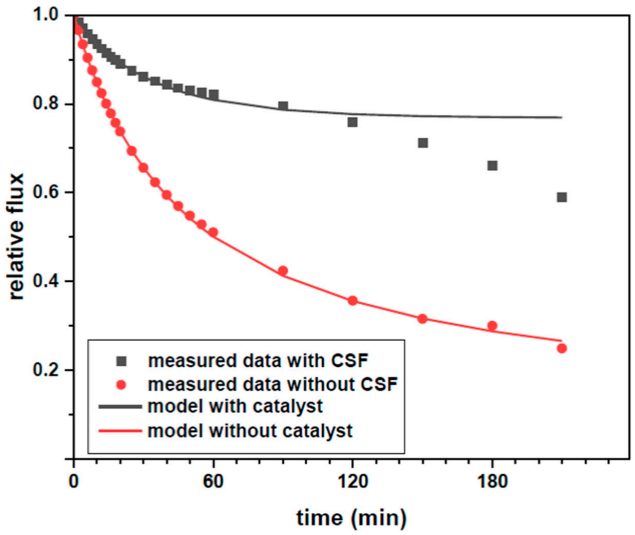

Figure 5. Comparison of change of relative flux in time for effluent with and without thermocatalyst; bullets indicate experimental points; lines correspond to an intermediate pore blocking model (Supplementary Materials).

3.5. Thermocatalytic Treatment of the NF Concentrate

A second way to integrate CSF with NF is to use thermocatalysis as a separate step after concentration, thus saving energy by reducing the volume of wastewater which needs to be heated. Therefore, we performed a new experiment in which 900 mL of wastewater effluent were concentrated to 180 mL by filtration at 6 bar over the Al_2O_3-doped silica membrane. The sample was sparked with BPA in order to reach a BPA concentration of ~10 mg L^{-1} after concentration. After concentration, 50 mL samples of the concentrate were treated at 50 °C with CSF at concentrations of 1, 2 and 10 g L^{-1} over 5 h. As can be seen in Figure 6, treatment with CSF thermocatalyst in a batch reactor causes 35% abatement of COD after 5 h of treatment. COD abatement does not change significantly by increasing CSF concentration from 1 to 10 g L^{-1}. This result is consistent with the fact that the dissolved organic matter consists of different types of chemical species, some of which are highly recalcitrant to degradation, such as part of the humic substances. On the other hand, the abatement of BPA increases following the concentration of CSF, as shown in Figure 7. However, these tests show also that the thermocatalyst is less efficient in the abatement of BPA in real matrixes, which contain large quantities of dissolved organic matter, than when it was tested with model solutions of BPA dissolved in deionized water.

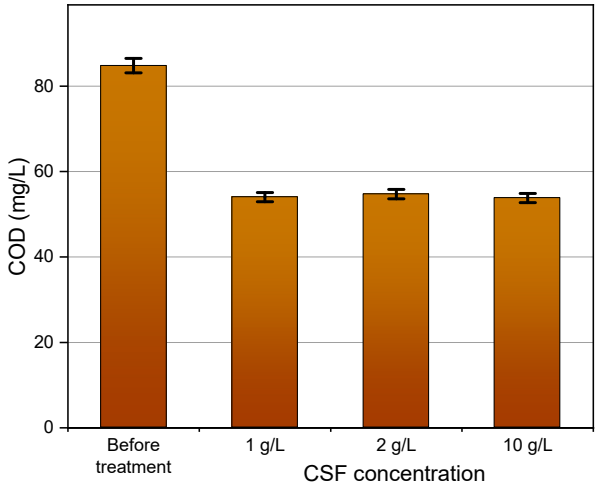

Figure 6. Chemical oxygen demand (COD) in the concentrated wastewater effluent before and after treatment with different amounts of CSF for 5 h.

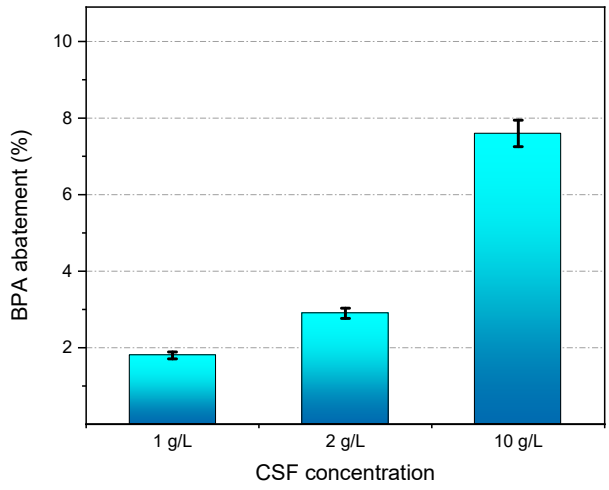

Figure 7. Abatement of BPA in the concentrated wastewater effluent after treatment with different amounts of CSF for 5 h.

4. Discussion

In this study, we presented a new method of water purification using the recently developed Al_2O_3-doped silica NF membrane combined with cerium-doped strontium ferrate (CSF), as thermocatalyst for the abatement of water pollutants. The new process was investigated in the degradation of bisphenol A (BPA), which is a common water contaminant with endocrine-disrupting activity. Concerning the NF membrane, we observed no impact of temperature on BPA rejection, which remains >98% at all the tested temperatures (30–60 °C). Instead, water permeance showed a twofold increment by increasing the feed temperature form 30 to 60 °C. Such temperature-permeance dependence in ceramic NF membranes can be explained by considering the change in solvent viscosity and that permeation in micropores occurs by a combination of viscous flow and activated transport [24]. Hence, the increase of the feed temperature is beneficial for membrane permeance and for the thermocatalytic abatement at the same time [20].

Two possible configurations were tested in this study, each of them with some specific advantages. Addition of CSF at the membrane feed during filtration allows for micropollutant abatement, while mitigating membrane fouling and improving the quality of the permeate. On the other hand, pre-concentration of the wastewater by nanofiltration allows for a strong reduction of the thermal energy needed for the thermocatalytic process, and decreases investment and running costs of the abatement step, since a smaller wastewater volume needs to be treated [26]. The two different configurations can be selected based on the type of wastewater, on its temperature, and on the presence of low-grade waste heat or renewable waste heat.

The experiments reported in this paper can also highlight some of the challenges for the implementation of this technology on a real scale. Firstly, non-toxic dissolved organic matter, which is typically present in wastewaters at concentrations much higher than the micropollutants, has a negative effect on both the water permeance of the membrane [27] and the thermocatalytic performances of CSF in the abatement of micropollutants. In this study, we show that CSF can degrade part of the dissolved organic matter and that, when added in the membrane feed, had also a positive impact on fouling. However, we also observed that CSF was able to degrade about 60% of BPA in deionized water after 3 h at 50 °C and less than 8% of BPA in concentrated wastewater (COD~85 mg L^{-1}) after 5 h at 50 °C. Therefore, thermocatalyst and process parameters should be optimized, taking into account the presence of non-toxic organic matter in real wastewater systems. A second challenge is the process upscaling. In this work, CSF was synthetized in a few grams batches by the solution-combustion method, which is notoriously not amenable to scale up. Nevertheless, Deganello et al. have indicated some strategies for large-scale synthesis of perovskites [27] and the industrial production of CSF is one of the tasks of the project NanoPerWater (EUREKA, Eurostars Cut-off 12, Project number: 113625). For the sake of comparison, all the thermocatalytic tests in this work were performed with dispersed CSF powders. Nevertheless, the recovery and reuse of the thermocatalyst is also a crucial aspect for this technology; especially when CSF is used in a separate abatement step after NF pre-concentration, and thus it cannot be retained by a membrane. For this reason, a possible implementation of this technology consists in the immobilization of the catalyst in a fixed-bed reactor for the abatement of micropollutants from wastewater effluent after pre-concentration over a NF membrane, which is indeed the scope of the recently funded NanoTheC-Aba project (JPI, 1st Aquatic Pollutants Joint Call 2020, Project number: ID 402). Concerning the economy of the new process, Ma et al. [14] have calculated that the Al_2O_3-doped silica NF membrane can operate at a specific energy consumption <0.15 kWh per m^3 of permeate, which makes this step potentially attractive when organic contaminants need to be removed from wastewater. Nevertheless, the thermocatalytic step requires at least 1.167 kWh (m^3 °C)$^{-1}$ for heating wastewater, making the overall process expensive, unless the wastewater stream to be treated already has a temperature suitable for CSF activation, or low-grade waste heat is available on site (which is the case for many industrial processes), or it is possible to exploit solar thermal energy.

5. Conclusions

For the first time, a thermocatalytic perovskite, namely Ce-doped strontium ferrate (CSF), was combined with a NF ceramic membrane for the treatment of wastewater. We showed that the addition of CSF to the membrane feed causes degradation of BPA and reduces BPA traces in the permeate. When the system was tested with a real wastewater effluent, CSF was able to reduce membrane fouling. From analysis of flux over time using different fouling models, it was found that the main fouling type occurring in our experiments is intermediate pore blocking. Our data show also that CSF can effectively degrade part of the non-toxic organic matter present in the water, which can explain its ability to mitigate membrane fouling. CSF can be also used to reduce the COD of wastewater after concentration by NF, although its ability to degrade BPA, and presumably the other micropollutants, is reduced by the scavenging effect of large concentrations of non-toxic organic matter, which also interacts with the reactive oxygen species generated by the thermocatalyst. Despite the abovementioned challenges, the new technology does not require light sources or additions of chemicals, contrary to other hybrid NF-advanced oxidation processes, e.g., those based on photocatalysis or Fenton technologies, respectively. Hence, integration of NF with thermocatalysis has the potential to rise as a new strategy for the treatment of wastewaters contaminated by micropollutants.

Supplementary Materials: The following are available online at https://www.mdpi.com/article/10.3390/membranes11080639/s1: Paragraph S1: Analysis of fouling models; Table S1: Results of R2 for each fouling method for filtration with and without catalyst.

Author Contributions: V.B. conceived the concept. K.J. and X.M. carried out materials synthesis and permeation tests. K.J., M.K.J., V.B. and V.M.C. analyzed data. K.J. wrote the paper with editorial contributions from V.B., M.K.J., V.M.C. and X.M. All authors have read and agreed to the published version of the manuscript.

Funding: This research was funded by the European Union's Horizon 2020 research and innovation program under the Marie Skłodowska-Curie grant agreement N. 765860.

Data Availability Statement: Data are contained within the article or Supplementary Materials.

Conflicts of Interest: The authors declare no conflict of interest.

References

1. Valbonesi, P.; Pro, M.; Vasumini, I.; Fabbri, E. Science of the Total Environment Contaminants of emerging concern in drinking water: Quality assessment by combining chemical and biological analysis. *Sci. Total Environ.* **2021**, *758*, 143624. [CrossRef] [PubMed]
2. Shahkaramipour, N.; Tran, T.N.; Ramanan, S.; Lin, H. Membranes with Surface-Enhanced Antifouling Properties for Water Purification. *Membranes* **2017**, *7*, 13. [CrossRef]
3. Chen, H.; Ku, J.; Wang, L. Thermal catalysis under dark ambient conditions in environmental remediation: Fundamental principles, development, and challenges. *Chin. J. Catal.* **2019**, *40*, 1117–1134. [CrossRef]
4. Werber, J.R.; Osuji, C.O.; Elimelech, M. Materials for next-generation desalination and water purification membranes. *Nat. Rev. Mater.* **2016**, *1*, 16018. [CrossRef]
5. Anderson, M.G.; Mcdonnell, J.; Ximing, C.; Cline, S.A.; Balance, W.W.; Rockstrom, J.; Daily, G.C.; Ehrlich, P.R.; Reidy, C.A.; Dynesius, M.; et al. The Challenge of Micropollutants in Aquatic Systems. *Science* **2006**, *313*, 1072–1077.
6. Xu, R.; Qin, W.; Tian, Z.; He, Y.; Wang, X.; Wen, X. Enhanced micropollutants removal by nanofiltration and their environmental risks in wastewater reclamation: A pilot-scale study. *Sci. Total Environ.* **2020**, *744*, 140954. [CrossRef] [PubMed]
7. Escalona, I.; Fortuny, A.; Stüber, F.; Bengoa, C.; Fabregat, A.; Font, J. Fenton coupled with nanofiltration for elimination of Bisphenol A. *Desalination* **2014**, *345*, 77–84. [CrossRef]
8. Li, C.; Sun, W.; Lu, Z.; Ao, X.; Li, S. Ceramic nanocomposite membranes and membrane fouling: A review. *Water Res.* **2020**, *175*, 115674. [CrossRef]
9. Wang, P.; Wang, F.; Jiang, H.; Zhang, Y.; Zhao, M.; Xiong, R.; Ma, J. Strong improvement of nanofiltration performance on micropollutant removal and reduction of membrane fouling by hydrolyzed-aluminum nanoparticles. *Water Res.* **2020**, *175*, 115649. [CrossRef]
10. Abdel-Fatah, M.A. Nanofiltration systems and applications in wastewater treatment: Review article. *Ain Shams Eng. J.* **2018**, *9*, 3077–3092. [CrossRef]

11. Farsi, A.; Malvache, C.; de Bartolis, O.; Magnacca, G.; Kristensen, P.K.; Christensen, M.L.; Boffa, V. Design and fabrication of silica-based nanofiltration membranes for water desalination and detoxification. *Microporous Mesoporous Mater.* **2017**, *237*, 117–126. [CrossRef]
12. García, N.; Purcell-milton, F.; Gun, Y.K. Recent progress and future prospects in development of advanced materials for nano fi ltration. *Mater. Today Commun.* **2020**, *23*, 100888. [CrossRef]
13. Chon, K.; Cho, J. Fouling behavior of dissolved organic matter in nanofiltration membranes from a pilot-scale drinking water treatment plant: An autopsy study. *Chem. Eng. J.* **2016**, *295*, 268–277. [CrossRef]
14. Ma, X.; Janowska, K.; Boffa, V.; Fabbri, D.; Magnacca, G.; Calza, P.; Yue, Y. Surfactant-assisted fabrication of alumina-doped amorphous silica nanofiltration membranes with enhanced water purification performances. *Nanomaterials* **2019**, *9*, 1368. [CrossRef] [PubMed]
15. Tsuru, T. Inorganic porous membranes for liquid phase separation. *Sep. Purif. Methods* **2001**, *30*, 191–220. [CrossRef]
16. Li, N.; Wang, X.; Zhang, H.; Zhang, Z.; Ding, J.; Lu, J. Comparing the performance of various nanofiltration membranes in advanced oxidation-nanofiltration treatment of reverse osmosis concentrates. *Environ. Sci. Pollut. Res.* **2019**, *26*, 17472–17481. [CrossRef]
17. Wang, J.L.; Xu, L.E.J.I.N. Advanced Oxidation Processes for Wastewater Treatment: Formation of Hydroxyl Radical and Application Advanced Oxidation Processes for Wastewater Treatment: Formation of Hydroxyl Radical. *Crit. Rev. Environ. Sci. Technol.* **2012**, *42*, 251–325. [CrossRef]
18. Arca-Ramos, A.; Eibes, G.; Feijoo, G.; Lema, J.M.; Moreira, M.T. Potentiality of a ceramic membrane reactor for the laccase-catalyzed removal of bisphenol A from secondary effluents. *Appl. Microbiol. Biotechnol.* **2015**, *99*, 9299–9308. [CrossRef]
19. Zielińska, M.; Cydzik-Kwiatkowska, A.; Bułkowska, K.; Bernat, K.; Wojnowska-Baryła, I. Treatment of Bisphenol A-Containing Effluents from Aerobic Granular Sludge Reactors with the Use of Microfiltration and Ultrafiltration Ceramic Membranes. *Water. Air Soil Pollut.* **2017**, *228*, 282. [CrossRef]
20. Janowska, K.; Boffa, V.; Jørgensen, M.K.; Quist-Jensen, C.A.; Hubac, F.; Deganello, F.; Coelho, F.E.B.; Magnacca, G. Thermocatalytic membrane distillation for clean water production. *NPJ Clean Water* **2020**, *3*, 1–7. [CrossRef]
21. He, Z.; Lyu, Z.; Gu, Q.; Zhang, L.; Wang, J. Ceramic-based membranes for water and wastewater treatment. *Colloids Surfaces A Physicochem. Eng.* **2019**, *578*, 123513. [CrossRef]
22. Deganello, F.; Tyagi, A.K. Solution combustion synthesis, energy and environment: Best parameters for better materials. *Prog. Cryst. Growth Charact. Mater.* **2018**, *64*, 23–61. [CrossRef]
23. Farsi, A.; Boffa, V.; Qureshi, H.F.; Nijmeijer, A.; Winnubst, L.; Christensen, M.L. Modeling water flux and salt rejection of mesoporous γ-alumina and microporous organosilica membranes. *J. Membr. Sci.* **2014**, *470*, 307–315. [CrossRef]
24. Tsuru, T.; Izumi, S.; Yoshioka, T.; Asaeda, M. Temperature Effect on Transport Performance by Inorganic Nanofiltration Membranes. *AIChE J.* **2000**, *46*, 565–574. [CrossRef]
25. Mora, F.; Karla, P.; Quezada, C.; Herrera, C.; Cassano, A. Impact of Membrane Pore Size on the Clarification Performance of Grape Marc Extract by Microfiltration. *Membranes* **2019**, *9*, 146. [CrossRef]
26. Miralles-Cuevas, S.; Oller, I.; Agüera, A.; Pérez, J.A.S.; Sánchez-Moreno, R.; Malato, S. Is the combination of nanofiltration membranes and AOPs for removing microcontaminants cost effective in real municipal wastewater effluents? *Environ. Sci. Water Res. Technol.* **2016**, *2*, 511–520. [CrossRef]
27. Oller, I.; Miralles-cuevas, S.; Agüera, A.; Malato, S. Monitoring and Removal of Organic Micro-pollutants by Combining Membrane Technologies with Advanced Oxidation Processes. *Curr. Org. Chem.* **2018**, *22*, 1103–1119. [CrossRef]

ISSN (online): 2446-1636
ISBN (online): 978-87-7573-810-6

AALBORG UNIVERSITY PRESS